European Journal of Operational Research 309 (2023) 1300–1315

Contents lists available at ScienceDirect

European Journal of Operational Research

journal homepage: www.elsevier.com/locate/ejor

Innovative Applications of O.R.

Electric aircraft charging network design for regional routes: A novel mathematical formulation and kernel search heuristic

Alan Kinene[a], Sebastian Birolini[b,*], Mattia Cattaneo[b], Tobias Andersson Granberg[a]

[a] Div. Communication and transportation Systems, ITN, Linköping University, Bredgatan 33, Norrköping 601 74, Sweden
[b] Department of Management, Information and Production Engineering, University of Bergamo, via 7 Pasubio 7b, Dalmine, BG 24044, Italy

ARTICLE INFO

Article history:
Received 21 November 2021
Accepted 7 February 2023
Available online 15 February 2023

Keywords:
Transportation
Electric aircraft
Network optimization
Regional routes
Kernel search

ABSTRACT

The uptake of electric aircraft appears faster today than predicted. Given the prominent electric aircraft technologies, short- and medium-haul routes are the ones that will benefit first, with the promise to revolutionize regional aviation at short notice. This paper proposes an optimization model to support the strategic design of charging networks for electric aircraft as a key enabling factor to prepare for and take full advantage of aviation electrification. The model, named *Electric Aircraft Charging Network for Regional Routes*, defines a network of airports and flight paths to optimally trade-off the number of charging bases (and associated investment costs) with connectivity and population coverage targets typical of regional routes serving remote regions. Due to computational challenges in large problem instances, we propose a Kernel Search heuristic and illustrate how it can deliver high quality solutions for large cases in a shorter computational time than the branch-and-cut algorithms. A real-world application to Sweden then demonstrates the practical insights of the proposed approach. We find that leveraging the many currently under-utilized regional airports has connectivity and investment benefits (on average +12.1% in number of origins covered, +5.8% in population coverage, and −7.3% reduction of travel times). Furthermore, increasing the maximum aircraft range on a single charge implies significantly fewer charging bases and more feasible travel options, thus favoring network resilience and granting higher flexibility for later planning stages.

1. Introduction

In the last decades, the rapid expansion of air transportation has boosted global mobility, international trade, and socio-economic development, while generating long-standing negative environmental effects. Before the brutal disruption of the transportation sector due to the COVID-19 pandemic, commercial aviation accounted for more than 11.0% of greenhouse gas emissions of all transport emissions, i.e., 2.4% of the global emissions[1] (3.6% in EU28 EASA, 2019), making the mitigation of air transportation's environmental burden among the most critical and controversial challenges of our times. Although the COVID-19 pandemic made the environmental burden less urgent because of the significant contraction in demand (and consequently aircraft movements), the air transportation industry is on the path to recovery to pre-pandemic levels (Grewe et al., 2021; Gudmundsson et al., 2021). Moreover, with post-pandemic stimulus initiatives mostly dedicated to advancing the digital and green transition of economy and society (OECD, 2021), the recovery period provides an unprecedented opportunity to rethink the aviation industry in a more sustainable way.

Traditional strategies to contain aviation's atmospheric and noise pollution have mostly involved the implementation of CO_2 trading schemes (e.g., EU ETS, Nava et al., 2018; CORSIA, Sharma et al., 2021), interventions to favor modal shift to other transportation modes such as high-speed rail,[2] and restrictions to the number of flight movements at congested hubs. Yet, these measures have been proven scarce and insufficient to achieve the ambitious middle-long decarbonization targets (e.g., D'Alfonso et al., 2016; Vespermann & Wald, 2011).

* Corresponding author.
E-mail addresses: alan.kinene@liu.se (A. Kinene), sebastian.birolini@unibg.it (S. Birolini), mattia.cattaneo@unibg.it (M. Cattaneo), tobias.andersson.granberg@liu.se (T.A. Granberg).

[1] EESI - The Growth in Greenhouse Gas Emissions from Commercial Aviation (2019).

[2] Reuters - French lawmakers approve a ban on short domestic flights. April 11, 2021.

https://doi.org/10.1016/j.ejor.2023.02.006

In parallel, significant efforts have recently been devoted to the development of sustainable aircraft technologies, especially towards electric aircraft (that is both all-electric and hybrid aircraft). Several aircraft manufacturers and startups have embarked on an intense electrification journey[3] and the uptake of electric aircraft appears faster today than predicted. Some of the pioneering aircraft models are *Alice*—an all-electric aircraft developed by the Israeli Eviation capable of an operating range of around 800 kilometers—, *ES-19* and the *ES-30*—electric aircraft prototypes developed by the Swedish Heart Aerospace characterized by an expected operating range of 200–800 kilometers depending on the aircraft configuration (all-electric vs. hybrid, and seat capacity) and time of deployment—, and *ZA10*—a 12-seater hybrid-electric aircraft developed by the US based Zunum Aero capable of an operating range up to 1127 kilometers. These models aim to be certified for commercial aviation in a short time, as early as 2024 (Baumeister et al., 2020; Eviation, 2021) with the potential to forthwith revolutionize regional aviation and short-haul markets at short notice (Justin et al., 2020)[4] Current estimates report that 15- to 20-seat battery-powered aircraft capable of an operating range of 400–500 kilometers will likely enter the market around 2030 (IATA, 2021; Reimers, 2018). The technological maturity of electric aircraft is also demonstrated by the fact that an increasing number of companies are expressing interest in procuring electric aircraft to complement their fleet (e.g., Finnair, Mesa Airlines), with some of them even placing orders (e.g., DHL express, Cape Air, United Airlines).

Overall, there are compelling advantages to the technological advancements in electric aviation. First, electric aircraft have the promise to drastically reduce both CO_2 and non-CO_2 emissions. Second, electric aircraft technology is expected to produce less noise—with a reduction of about 36%—compared to current best-in-class jet-fuel aircraft technology (see Schäfer et al., 2019). Third, a significant reduction in maintenance costs because of the greater simplicity of electric motors compared to combustion engines (Patterson et al., 2016). On the other hand, the adoption of electric aircraft comes with a number of challenges. A major concern is related to battery technology; current technology would require the use of several sets of batteries over the life-cycle of an aircraft—causing increased capital and maintenance costs. Additionally, the first generations of electric aircraft will likely be characterized by higher weight per unit of stored energy—limiting the size and the operating range of fully-battery-powered aircraft.[5] Third, from a planning perspective, the operation of electric aircraft poses challenges spanning strategic infrastructure-related questions, network design, and tactical scheduling and routing problems. In particular, a key issue today is the development of assessment methods and planning tools that capture features of viable electric aircraft technology in the near- to mid-term, with the aim to support the strategic planning of dedicated and enabling infrastructures.

The implications of electric aircraft on airline operations are significant and motivate an assessment of their impact not only on existing aviation business models and markets, but also on new aviation markets such as on-demand services (Justin et al., 2020; Willey & Salmon, 2021). As a middle ground, the fast development of small size electric aircraft technologies represents a major opportunity to profitably serve thin markets that today cannot sustain scheduled air services operated using medium- and wide-body aircraft. A specific example of thin markets is regional routes serving remote regions. A number of subsidy schemes are currently in place in different countries to support connectivity to/from such regions, such as the Essential Air Services (EAS) program in the United States, the Public Service Obligations (PSO) system in Europe, the Remote Air Service Subsidy (RASS) scheme in Australia, the Rural Air Services (RAS) program in Malaysia, and the Peruvian PSO (Programa de Integración Amazónica por vía Aérea) scheme (see for a review Fageda et al., 2018). From a welfare-perspective, these schemes aim to incentivize the provision of air services while suitably trading-off the conflicting goals of maximizing accessibility and minimizing public expenses. The characteristics of regional routes make them among the first candidates to reap the benefits of aircraft electrification. Regional routes typically range between 200 and 800 kilometers (Fageda et al., 2018; Graham, 1997), which perfectly fits the expected operating range of the first commercial electric aircraft. Additionally, small-size electric aircraft can operate at airports with shorter runways (e.g., about 800 meters, TrafikAnalys, 2020) and thus could take advantage of existing, underutilized airports and airfields to foster regional connectivity. Eventually, the deployment of electric aircraft is expected to lower operating costs, which in turn would contribute to the profitability of thin routes and thus reduce the need for public subsidy. Additionally, the short-term costs for the use of electric aircraft are still uncertain, but it is likely that governments might even be willing to increase subsidies, if this will decrease the environmental cost of increased air connectivity.

Despite the rapidly growing literature that investigates aircraft electrification and implementation (see Barzkar & Ghassemi, 2020; Sayed et al., 2021, for a review), particularly in the realm of Urban Air Mobility (see Rajendran & Srinivas, 2020, for a review), literature is way more scant concerning the use of electric aircraft in a regional context, especially with respect to their strategic planning or the planning of related infrastructure (e.g., location of charging bases) (Salucci et al., 2020; Trainelli et al., 2021). Yet, similar to the set of studies advanced during the last decade to support the fast-growing adoption of electric ground vehicles (e.g., Hiermann et al., 2016; Hosseini & MirHassani, 2015; Hung et al., 2022; Kınay et al., 2021; Mak et al., 2013) investment efforts regarding electric aircraft are capital intensive and cannot be addressed in isolation. Instead, they need to be planned carefully and in an integrated network-wide fashion to suitably prioritize interventions at certain airports. In particular, at focal airport charging bases,—which we also refer to as charging hubs—that is, airports that are pivotal to the network's connectivity due to their central role in terms of passenger paths (trips), resulting in a significant number of aircraft movements. These focal charging bases will likely require a significant amount of power, thus necessitating significant infrastructure updates to the electricity grid (Schwab et al., 2021; Trainelli et al., 2021) that need to be addressed beforehand.

In this paper, we propose a modeling framework—referred to as *Electric Aircraft Charging Network for Regional Routes (EACN-REG)*—that defines the network of airports and the location of focal charging bases, to optimally trade-off the number of charging bases (and associated implementation costs) with connectivity and population coverage targets typical of regional routes. Identifying the focal charging bases within a network of airports to expand air connectivity needs to be done before the electric aviation industry can take off. In this respect, the model's ability to design a network with appropriate focal charging bases constitutes an essential part of the electric aviation strategic road-map: that is, to coordinate investment efforts to reduce construction lead time at focal airports, and ultimately provide a strong infrastructure foundation to support a fast roll-out of electric aircraft technology.

In summary, this paper makes the following contributions:

[3] In the third quarter of 2021, there were more than 215 active projects on electric-propelled aircraft globally (Roland Berger - Environmentally-friendly air travel continues to grow. September 10, 2021).

[4] On the contrary, the deployment of electric aircraft on long-haul markets will require longer time (Åkerman et al., 2021).

[5] Current energy equivalence: 1 kilogram of fossil fuel is equivalent to what can be stored in 10–13 kilograms of batteries (Rohacs & Rohacs, 2020).

1. It develops a novel optimization model to support the strategic planning of electric aircraft networks for regional routes. The model is formulated as a multi-objective uncapacitated facility location problem that optimizes regional connectivity while minimizing the number of charging bases. Instead of restricting to smooth radius/range coverage-like constraints, we account for multi-step aircraft operations through a set of routing feasibility constraints. The formulation of the routing feasibility constraints requires the calculation of the shortest-path distance from each airport to a charging base, which constitutes a novel feature of the model. We tighten the model formulation through sets of valid inequalities, which allow solving the model using off-the-shelf branch-and-cut solvers for small- to mid-size instances in reasonable computation times.
2. It proposes a Kernel Search Heuristic to efficiently solve large-scale instances. Given the NP-hardness of the original problem, we develop a tailored Kernel search solution approach that exploits the structure of the problem. We develop a kernel initialization strategy based on network centrality and extend the basic kernel search (Angelelli et al., 2007) to allow for the recombination of buckets in multiple iterations to better capture correlations among items (airports). Through a comprehensive computational study using randomly-generated instances inspired from real-world data, we investigate the performance of the proposed heuristic method, showing how it can consistently achieve near-optimal solutions in less computational time than directly solving the original problem with branch-and-cut.
3. It demonstrates the benefits and practical insights of the proposed modeling approach considering a real-world case study. We take Sweden as an exemplary case study for two main reasons. First, electric propulsion is suitable for Sweden because of its geographical setup that could benefit from short-haul flights to avoid physical barriers and connect remote areas more efficiently. Second, Sweden like other Nordic countries such as Norway and Denmark is well-positioned as a pioneer in the adoption of electric aircraft. It is among the world-leading countries in the transition to renewable energy.[6] Moreover, it has a well-structured network of short field airports that could be leveraged to expand regional connectivity. In our case study, we show how the model can guide decision-making by testing the impact of the available number of airport candidates on connectivity and required number of charging bases, and testing the impact of aircraft range on connectivity requirements.

The remainder of the paper is organized as follows. Section 2 describes the formulation of the proposed EACN-REG model. In Section 3, we present formulation strengthening of the model and a Kernel Search heuristic to tackle the challenges of solving real-world instances. The results of a computational experiment using randomly generated data and the application of the EACN-REG to a real-world case study are presented in Sections 4 and 5, respectively. We then summarize our contributions and outline future research directions in Section 6.

2. Optimization model

In this section, we present the formulation of the proposed Electric Aircraft Charging Network for Regional Routes (EACN-REG) model.

[6] Sweden has undertaken strong medium- to long-term commitment to reduce carbon emissions of regional aviation significantly, aimed to operate only zero-carbon domestic flights by 2030.

2.1. Problem setting

The EACN-REG model aims to design an airport network of charging bases for electric aircraft operations in the context of regional routes. Specifically, it selects the airports to be used as charging bases from a set of candidate airports while considering a maximum flight range on a single charge, ensuring multi-step routing feasibility and maximizing service connectivity for the population area under study. We illustrate the problem with a small synthetic example (see Fig. 1).

The model takes as input a grid with two main components: the grid cells that partition the population area defined as a set $\mathcal{K}$ indexed by k, and candidate airports defined as set $\mathcal{N}$ indexed by i and j. In practice, these may include currently used commercial airports and regional or military airports/airfields with a runaway length that can accommodate electric aircraft operations. We further define the set of edges $\mathcal{E}$ to represent potential directional flight edges between airports. For example, in Fig. 1, we have a grid with 28 grid cells (e.g., k_1 and k_2), 4 airports (i.e., 1, 2, 3, 4) connected by 4 flight edges (i.e., (1,2), (1,3), (2,3), and (3,4)). We define the flight distance d_{ij} for each edge (i, j)—computed as the geodesic distance between the two airports. Note that, as further explained in Section 5, this distance can be adjusted to account for safety requirements such as energy reserves to divert to an alternate airport and other reserves. We then consider a maximum travel distance on a single charge (τ) to capture the range limitation of electric aircraft. Accordingly, edges with $d_{ij} > \tau$, for example edge (2,4) in Fig. 1, are not included in set $\mathcal{E}$.

To account for regional connectivity in the model, we define a set of target destinations ($\mathcal{D}$). In practice, these are major cities or hubs that population areas $k \in \mathcal{K}$ need to be connected to. We also define a set of feasible paths $\mathcal{P}$ from any airport to the target destinations. Paths are defined as a sequence of flight edges. For example, in Fig. 1, assuming airport 4 as the destination airport within the final destination cell, we can generate four paths from the rest of the airports as an edge or a sequence of adjacent edges: $p_1 = \{(1,3),(3,4)\}$, $p_2 = \{(1,2),(2,3),(3,4)\}$, $p_3 = \{(2,3),(3,4)\}$, and $p_4 = \{(3,4)\}$. Note that additional paths are possible. Paths are used to map possible ways that passengers can travel in the airport network and do not necessarily coincide with aircraft routings—which will be defined at later stages of the planning process. Indeed, flights along a path may be operated by different aircraft. Then, to account for the connectivity of each origin k, we define subsets $\mathcal{P}_k^d$ of possible paths that passengers from k can travel to reach destination d. Not all paths represent reasonable travel options for all origin cells due to the geographical setup and the ground transportation infrastructure, which may affect ground access to the airports and cause inconvenience due to detours. For example, in Fig. 1, we assume that the population from k_1 can utilize paths from airport 1 and 2 (i.e., p_1, p_2 from airport 1 and p_3 from airport 2), while that from k_2 can only utilize one path (p_3) from airport 2 because accessing any other airport would take too much time—compared to directly going to the target destination by ground transportation or within a reasonable maximum access time thresholds. The definition of P_k^d allows us to flexibly capture various connectivity requirements. In the case of remote regions, planning authorities typically state a maximum total travel time as a requirement for connectivity to target destinations (Bråthen & Eriksen, 2018; Williams & Pagliari, 2004)—e.g., 4 hours in Sweden—thus providing a clear filtering criteria for the paths. The filtering of paths is part of the pre-processing of set $\mathcal{P}$ and $\mathcal{P}_k^d$, which avoids difficult-to-model constraints and yields strong formulations.

The model has five main variables: (1) a binary variable (y_i) indicating the selection of an airport i as a charging base; (2) a continuous variable (ρ_i) computing the shortest path distance from any airport i to an airport being selected as a charging base; (3) a

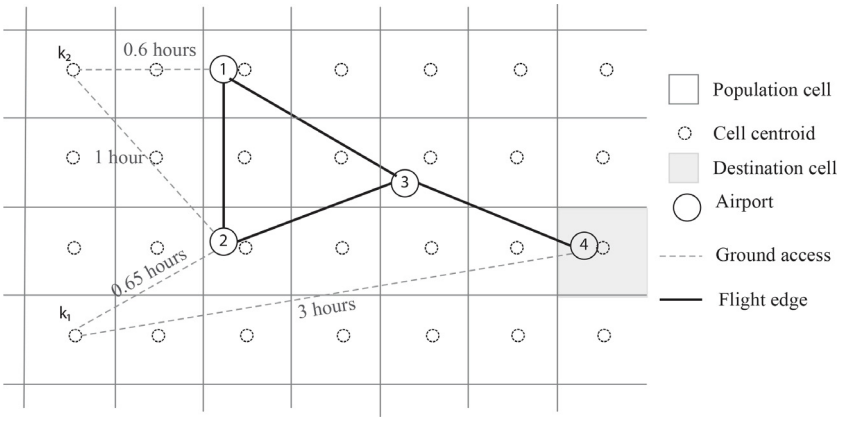

Fig. 1. An illustration of the modeling elements.

binary variable (z_{ij}) modeling the feasibility of a given flight edge—as a function of the location of the charging bases and the travel range; (4) a binary variable ψ_p indicating if path p can be used (i.e., all the included flight edges are feasible); and (5) a binary variable ϕ_k^d indicating whether region k is connected to destination d.

Based on this modeling setup, the EACN-REG optimizes two main objectives: (1) maximization of regional connectivity; (2) minimization of the investment-cost for charging bases. These objectives capture the regional planners' objective of ensuring connectivity for the population to the main destinations and the aspect of limited availability of funds for investment. Additionally, other objectives could be considered (e.g., in a lexicographic fashion) to select among the possibly many alternative optimal solutions. For example, a planner could maximize the number of feasible paths to provide flexibility in (later) tactical planning phases, such as flight scheduling and fleet assignment, or select the solution that minimizes the total travel time across all origins.

The EACN-REG is formulated as a strategic network-based problem that does not require explicit assumptions regarding the very uncertain demand (especially in a regional context and markets that are not currently served by air transportation) and fleet size and composition. Decisions of where to locate focal charging bases (with aircraft charging stations) are indeed costly and span a long-time horizon; at the same time, charging facilities need to be provided before observing the actual demand. Note that the EACN-REG focuses on the planning of large charging hubs. Yet, having a single or a few chargers at each airport (e.g., for safety reasons) can possibly be accommodated without major investments or network-wide considerations. Thus, the precise number of chargers at each airport can be better appraised at a more tactical level of the planning process, when scheduling and fleet sizing decisions will be more carefully addressed.

2.2. Mathematical formulation

We now introduce the complete notation for the EACN-REG model in Table 1 and formulate it mathematically.

(EACN-REG) Objectives :

$$O_1 = \max \quad \mu_1 \sum_{d\in\mathcal{D}} \sum_{k\in\mathcal{K}} \pi_k \phi_k^d \tag{1}$$

$$O_2 = \min \quad \mu_2 \sum_{i\in\mathcal{N}} c_i y_i \tag{2}$$

Constraints :

$$\text{s.t.} \quad \rho_i = \mathcal{SP}(y_i, \rho_{j|j\in\mathcal{N}_i}) \qquad \forall i \in \mathcal{N} \tag{3}$$

$$d_{ij} + \rho_i + \rho_j - M^3(1 - z_{ij}) \leq \tau \qquad \forall (i,j) \in \mathcal{E} \tag{4}$$

$$\psi_p \leq z_{ij} \qquad \forall (i,j) \in \mathcal{E}_p, \forall p \in \mathcal{P} \tag{5}$$

$$\phi_k^d \leq \sum_{p\in\mathcal{P}_k^d} \psi_p \qquad \forall k \in \mathcal{K}, \forall d \in \mathcal{D} \tag{6}$$

$$y_i \in \{0,1\}, \rho_i \in \mathbb{R}^+ \qquad \forall i \in \mathcal{N} \tag{7}$$

$$z_{ij} \in \{0,1\} \qquad \forall (i,j) \in \mathcal{E} \tag{8}$$

$$\psi_p \in \{0,1\} \qquad \forall p \in \mathcal{P} \tag{9}$$

$$\phi_k^d \in \{0,1\} \qquad \forall k \in \mathcal{K}, \forall d \in \mathcal{D} \tag{10}$$

Eqs. (1) and (2) form a two-part objective function: Eq. (1) maximizes regional connectivity expressed as the sum of the population of covered origins with respect to all destinations, and Eq. (2) minimizes the total investment costs for charging stations at airports. Note that for the first objective, alternative connectivity targets could be flexibly accounted for in our modeling framework depending on the planning focus. For instance, regions are typically associated with connectivity targets that could be formulated as coverage constraints in terms of variable ϕ_k^d, including tailored requirements for each k and d, e.g., varying connectivity target times for the possibility of travel from the population areas to a specific destination. Similarly, detailed knowledge about airport investment costs and a given budget could allow the formulation of the second objective as a constraint and suitably prioritize budget allocation. Constraints (3) compute the shortest path to a charging base for each airport. Mathematically, $\mathcal{SP}(y_i, \rho_{j|j\in\mathcal{N}_i})$ can be stated as follows:

$$\mathcal{SP}\left(y_i, \rho_{j|j\in\mathcal{N}_i}\right) = \min\left(M^1(1-y_i), \min_{j\in\mathcal{N}_i}(d_{ij}+\rho_j)\right) \tag{11}$$

where M^1 is a large enough parameter. Eq. (11) is non linear but it can be conveniently linearized, as later illustrated in this section. Additionally, note that, under a reasonable assumption of symmetry, such that $d_{ij} = d_{ji}$, ρ_i represents the shortest path to and from a given airport—which turns useful in the formulation of the next constraint.[7] Constraints (4) compute the feasibility of each edge

[7] We could relax this assumption but this would require the definition of two separate variables, i.e., ρ_i^{in} and ρ_i^{out}, to capture the shortest path from a charging base to airport i and the shortest path from i to a charging base, respectively.

Table 1
Model notation.

Inputs: sets & parameters	
$\mathcal{N}$	set of airport nodes, indexed by i and j
$\mathcal{N}_i$	set of airport nodes adjacent to node i, i.e., $j \in \mathcal{N}$ such that $d_{ij} \leq \tau$ and $i \neq j$
$\mathcal{E}$	set of flight edges, indexed by (i, j)
$\mathcal{K}$	set of population areas, indexed by k
$\mathcal{P}$	set of paths, indexed by p
$\mathcal{D}$	set of destinations, indexed by d
$\mathcal{P}_k^d$	subset of paths from population area k to destination d
$\mathcal{E}_p$	subset of flight edges in path p
d_{ij}	travel distance between i and j
τ	maximum travel range on a single charge
c_i	cost of activating node i as a charging base
π_k	population living in k
μ_1, μ_2	weights of the two objectives in the objective function
Variables	
$y_i \in \{0, 1\}$	$= 1$ if node i is activated as a charging base
$z_{ij} \in \{0, 1\}$	$= 1$ if flight edge (i, j) is feasible
$\rho_i \in \mathbb{R}^+$	value of the shortest path from i to a charging base
$\psi_p \in \{0, 1\}$	$=1$ if path p can be used
$\phi_k^d \in \{0, 1\}$	$=1$ if area k is covered w.r.t. destination d

by taking into account the maximum aircraft range (on a single charge) and the location of charging bases. An edge (i, j) is feasible if an aircraft can make a journey through it on a single charge, that is, the total journey distance from a charging base to a charging base does not exceed the maximum travel range. Despite formulating the problem at a strategic level and not explicitly solving the aircraft routing problem, Constraints (4) allow us to suitably consider the feasibility of multi-step journey/routing on a single charge. To operate edge (i, j), a given aircraft needs first to get from a charging base to i, travel through (i, j) and then continue to a charging base, such that the overall distance traveled is lower than the range. Given the length d_{ij} of (i, j) and shortest path distances to/from a charging base from both i and j, Constraints (4) formulate the minimum total routing distance through (i, j) as $\rho_i + d_{ij} + \rho_j$ and leverage big-M parameter M^3 to set z_{ij} equal to 0 whenever $\rho_i + d_{ij} + \rho_j > \tau$. Constraints (5) define the feasibility of any given path from the feasibility of all its edges from the feasibility of all its edges. A path is not usable (i.e., $\psi_p = 0$) if any of its edges is not feasible. Constraints (6) then force the coverage variables ϕ_k^d equal to zero when there is no feasible path from k to d, i.e., all paths in $\mathcal{P}_k^d$ are unfeasible. Finally, Constraints (7)–(10) define the domain of the variables. We now clarify how Eq. (11) can be reformulated by a set of linear inequalities in Proposition 1.

Proposition 1. *Let w_{ij} be one if the shortest path for node i goes through node j. Let χ_i be one if no feasible path from node i to a charging station exists. Let M^2 be a sufficiently large big-M parameter. The following linear inequalities can be used to equivalently replace Eq. (11).*

$$\rho_i \leq M^1(1 - y_i) \qquad \forall i \in \mathcal{N} \tag{12}$$

$$\rho_i \leq d_{ij} + \rho_j \qquad \forall j \in \mathcal{N}_i, \forall i \in \mathcal{N} \tag{13}$$

$$\rho_i \geq d_{ij} + \rho_j - M^2(1 - w_{ij}) \qquad \forall j \in \mathcal{N}_i, \forall i \in \mathcal{N} \tag{14}$$

$$\rho_i \geq M^1 \chi_i \qquad \forall i \in \mathcal{N} \tag{15}$$

$$\sum_{j \in \mathcal{N}_j} w_{ij} + y_i + \chi_i = 1 \qquad \forall i \in \mathcal{N} \tag{16}$$

Proof. See Appendix A.

Constraints (12)–(16) calculate the shortest path distance from node i to a charging base, or set it equal to M^1 if there is no charging base within that given threshold.[8] Constraints (12) ensure that if airport i is activated as a charging base, its shortest path value becomes zero. Otherwise, constraints (13)–(14) (along with (16)) implements the calculation of $\min_{j \in \mathcal{N}_i}(d_{ij} + \rho_j)$, that is, the shortest path from i to an airport activated as a charging base. This is done recursively, by taking the minimum of the sum of the distance between i and j (d_{ij}) and the shortest path from j (ρ_j), across all adjacent nodes to i, i.e., $j \in \mathcal{N}_i$. Specifically, constraint (13) imposes an upper bound on ρ_i, forcing it to be lower or equal to the sum of the distance from i to any adjacent airport j (d_{ij}) and the shortest path from that adjacent airport. Through parameter M^2, Constraints (14) imposes a lower bound on ρ_i that is equal to the minimum shortest path from i. To further clarify on the shortest path calculation, a simple illustrative example is reported in Appendix B. Adding variable χ_i to Constraints (16) and considering Constraints (15) force ρ_i to be equal to M^1 if there is no path to a charging base lower than M^1, which occurs, for example, in the case of disconnected sub-networks, as illustrated in detail in Appendix C.

3. Solution methods

The EACN-REG model can be seen as an extension of the classical maximum coverage uncapacitated location problem—a well known NP-hard problem (Church & ReVelle, 1974; Cornuéjols et al., 1991; Daskin, 2011)—with additional complexities due to the shortest path calculation and coverage constraints through the use of composite path variables. As such, it is very challenging to solve for real-world instances via direct implementation of exact branch-and-cut (B&C) algorithms provided by commercial solvers. In this section, we discuss methods to solve the EACN-REG for realistic problem sizes. We first discuss the strengthening of the model formulation in Section 3.1, which, as we shall see in Section 4, allows to consider exact optimization methods to solve small- to mid-size

[8] Note that Constraints (12) and (13) are not strictly needed and could be lifted, i.e., Constraints (3) could be formulated as a greater than or equal to inequality. Indeed, Constraints (14)–(16) suffice to set a lower bound on ρ_i equal to the shortest path to a charging base. Yet, the presentation of the model with these constraints facilitates the illustration of the shortest path calculation. Additionally, they serve as valid inequalities and defining an explicit upper bound on ρ_i helps tighten the model formulation, as better illustrated in Section 3.1.

instances, and then present a Kernel Search heuristic to solve the largest instances (Section 3.2).

3.1. Formulation strengthening

3.1.1. Tightening of big-M parameters

First, the big-M parameters need to be accurately set in order to tighten the model relaxation and accelerate the convergence of branch-and-cut algorithms. Setting a tight upper bound to ρ_i (i.e., M^1) enables to tighten the big-M parameters in the formulation and prevent issues associated with large big-M parameters.[9] Let us note, first, that in our model we leverage the variables ρ_i to enforce feasibility of edges adjacent to i. Hence, the tightest M^1 parameter value can be defined by identifying the smallest value of ρ_i such that any edge linked to i, i.e., (i, j) and (j, i) is infeasible. Such value is provided in the following proposition (Proposition 2).

Proposition 2. *Given an airport i with no charging base (i.e., $y_i = 0$), then any (i, j) or (j, i) is infeasible if and only if $\rho_i > \tau - \min_{j' \in \mathcal{N}_i} d_{ij'}$.*

Proof. See Appendix A.

From Proposition 2, we can thus define the tightest node specific big M^1 parameters as follows:

$$M_i^1 = \tau - \min_{j' \in \mathcal{N}_i} d_{ij'} + \epsilon \tag{17}$$

with ϵ being a small positive number, without cutting off any feasible solution for the key decision variables y_i and z_{ij}. As ρ_i is bounded above, we can then define big-M parameters M^2 and M^3 for each edge (i, j) as follows:

$$M_{ij}^2 = d_{ij} + \tau - \min_{i' \in \mathcal{N}_j} d_{ji'} + \epsilon \tag{18}$$

$$M_{ij}^3 = d_{ij} + \tau - \min_{j' \in \mathcal{N}_i} d_{ij'} - \min_{i' \in \mathcal{N}_j} d_{ji'} + 2\epsilon \tag{19}$$

whose validity directly follows from Constraints (14) and (4), respectively.

3.1.2. Tightening constraints

Additionally, we consider the following set of valid inequalities, which proved effective for enhancing the solvability of the EACN-REG model:

$$\rho_i \geq \min\left(\min_{j \in \mathcal{N}_i} d_{ij}, M_i^1\right)(1 - y_i), \qquad \forall i \in \mathcal{N} \tag{20}$$

$$z_{ij} \leq 1 - \chi_i, \qquad \forall (i, j) \in \mathcal{E} \tag{21}$$

$$z_{ij} \leq 1 - \chi_j, \qquad \forall (i, j) \in \mathcal{E} \tag{22}$$

Constraints (20) enforce a lower bound on the shortest path value at each airport i—when it is not selected as a charging base (i.e., $y_i = 0$)—equal to the minimum between the distance to the closest adjacent airport and the shortest path threshold provided in Eq. (17). Constraints (21) and (22) link variables z_{ij} and χ_i and χ_j, respectively. Their validity directly follows from Constraints (15)—according to which χ_i is set equal to 1 if and only if the shortest path value to a charging base from i is higher than M_i^1—and Proposition 2.

[9] Let us consider, for example, Constraints (14). If M^2 is very large (i.e., $M^2 \gg d_{ij} + \rho_j$), then the model can set $y_i, \chi_i = 0$ and set some $w_{ij} > 0$ such that $\sum_{j \in \mathcal{N}_i} w_{ij} = 1$, while keeping ρ_i very low or zero.

3.1.3. Binary relaxation

We observe that, due to the structure of the problem, we can relax variables ϕ_k^d and ψ_p replacing the associated binaries with continuous variables bounded between 0 and 1, i.e., $\psi_p \in [0, 1] \cap \mathbb{R}^+$ and $\phi_k^d \in [0, 1] \cap \mathbb{R}^+$. Constraints (6) force ϕ_k^d equal to 0 if no path in P_k^d is feasible. If, on the contrary, there is at least one feasible path p (i.e., $\psi_p = 1$) from k to destination d, then the model will automatically set ϕ_k^d equal to 1 (its upper bound) as this adds to the objective function. For variables ψ_p, we have that Constraints (5) set them equal to 0 if at least one edge belonging to the path p is not activated. To ensure that ψ_p takes an integer value in the model relaxation when the path is feasible, we then add the following constraints:

$$\psi_p - \sum_{(i,j) \in \mathcal{E}_p} z_{ij} \geq 1 - |\mathcal{E}_p|, \qquad \forall p \in \mathcal{P} \tag{23}$$

which forces ψ_p equal to 1 when all its edges are feasible. Similarly, we can add the following constraints to set z_{ij} equal to 1 whenever feasible:

$$d_{ij} + \rho_i + \rho_j + M_{ij}^4 z_{ij} \geq \tau, \qquad \forall (i, j) \in \mathcal{E} \tag{24}$$

where $M_{ij}^4 = \tau - d_{ij}$. This, in turn, accelerates the convergence of the B&C search and in particular the proof of optimality.

3.2. Kernel search heuristic

Kernel Search (KS) is a general heuristic method designed to solve Mixed Integer Linear Problems (MILP) with binary variables—modeling the selection of items—as well as other integer and continuous variables. Angelelli et al. (2007) was first to introduce the basic KS, and its iterative variant to solve a portfolio optimization problem. The main idea of the basic KS is to obtain a possibly high quality solution by not considering all the items at once but rather starting from a small set of promising items—forming an initial *kernel*—and exploring the possibility to add more items by solving a sequence of moderate size MILP sub-problems. Items not belonging to the initial kernel are partitioned into subsets called *buckets*. Then, a sub-problem is solved for each bucket by restricting it to its items and those in the present kernel, to identify possible new items to extend the kernel. The iterative variant of the KS includes an extra iteration(s) that revisits the buckets to further extend the kernel. Guastaroba et al. (2017) further extended the basic KS to the Adaptive Kernel Search (AKS) algorithm, with a kernel-update adaptive scheme that also considers removal of items from the kernel.

Since its original development, KS has been applied to a wide range of combinatorial problems, encompassing a multi-dimensional knapsack problem (Angelelli et al., 2010; Lamanna et al., 2022), facility location problems (Filippi et al., 2021; Guastaroba & Speranza, 2012; 2014; Yang et al., 2019), and the index tracking problem (Filippi et al., 2016; Guastaroba & Speranza, 2012). The literature shows that the KS is a powerful tool for obtaining high quality solutions for complex MILPs with a similar structure as our EACN-REG—that is, mixed-integer linear problems defined on binary variables modeling item selection, together with other integer or continuous variables related to the selected variables (Maniezzo et al., 2021). Indeed, the EACN-REG is characterized by the selection of a subset of focal charging airports out of a pool of airport candidates (defined by binary variable y_i) with high network synergies and interaction captured through other variables for link feasibility, shortest path, path selection, and population area connectivity. The effective performance of KS algorithms significantly depends on two critical choices (Angelelli et al., 2010). The first is the building of the initial kernel—the criterion and size. The idea is to find a criterion such that the items that are more

likely to belong to the optimal solution are part of the initial kernel as such would accelerate the convergence of the algorithm. The second is the generation of buckets and the iterating scheme. Indeed, we would like to have small buckets for quicker updates of the kernel, but also heterogeneous and large to capture correlation among items. Note that this is a very important aspect in our model as we allow for multi-step aircraft operations that lead to interactions among airports.

We now present our kernel search algorithm, referred to as EACN-KS, by clarifying the construction of the kernel, the buckets, and summarizing the iterative algorithm.

3.2.1. Construction of the initial kernel

Previous papers (e.g., Angelelli et al., 2007; Filippi et al., 2021) solved the continuous relaxation of the original problem to inform the selection of initial kernel items. In our case, this approach proved ineffective because of the resulting loose relaxation of the EACN-REG—under which most of the y_i variables are set to 0, especially when considering large values of τ (i.e., long ranges). Therefore, given an initial kernel size $\bar{s}$, we devise a problem tailored centrality-based approach ($INIT(\mathcal{N}, \mathcal{P}, \mathcal{K}, \bar{s})$) to build the initial kernel (defined as $\mathcal{S}$). For each airport $i \in \mathcal{N}$, $INIT(\mathcal{N}, \mathcal{P}, \mathcal{K}, \bar{s})$ computes the number of origins $k \in \mathcal{K}$ that could be served based on the paths $p \in \mathcal{P}$ that go through it, then ranks the airports in descending order and selects the top $\bar{s}$ as part of the initial kernel.

3.2.2. Construction and exploration of the buckets

In our KS based heuristic, we randomly partition the remaining airports into buckets b of size $\bar{b}$ (with possible exception of the last one). We find a good bucket size $\bar{b}$, by experimentation. Additionally, we implement a modified version of the iterative KS where at the start of each iteration, we re-build the buckets from those remaining items/airports outside the kernel. This allows us to capture additional correlations among airports, which could further improve the incumbent solution. For example, let us assume that both airport 1 and airport 3 need to be activated to enable a given crucial path (e.g., serving a very remote area). Let us further assume that both airports are not in the kernel and their mutually exclusive activation does not improve the incumbent solution. If both airports are in separate buckets—which are sequentially explored by the heuristic—the correlation between these airports is not captured and neither airport will be added to the kernel (and consequently to the optimal solution). Instead, if airport 1 and airport 3 belong to the same bucket, they may both be added to the kernel as their joint contribution could allow serving an extra region and improve the solution. Hence, recombining buckets through multiple iterations helps accounting for this aspect.

3.2.3. Iterative algorithm

We now summarize the full iterative procedure in Algorithm 1. The EACN-KS takes as input the set of all airports $\mathcal{N}$, the maximum number of iterations $iter^{\max}$, the kernel size $\bar{s}$, the bucket size $\bar{b}$, and the maximum run time $T^{\max}$. In the initialization step, we build the initial kernel $\mathcal{S}$ of very promising airports for the location of charging bases using $INIT(\mathcal{N}, \mathcal{P}, \mathcal{K}, \bar{s})$, and set the incumbent objective value z^* and the iteration count $iter$ to zero.

We then extend the initial kernel through a series of iterations ($\leq iter^{\max}$) where we evaluate a sequence of buckets. At the start of each iteration, the set of non-kernel airports $\mathcal{U}$ is partitioned into buckets of size $\bar{b}$ forming a set of buckets $\mathcal{B}$. For each bucket, we solve a restricted version of the original model denoted as $EACN\text{-}REG^*(\mathcal{S} \cup b, z^*)$, which is obtained by editing the original model as follows: (1) charging bases can only be selected among a restricted set of airports given by the union of the kernel items and items belonging to the bucket under consideration, i.e., $\mathcal{S} \cup b$—note that, to capture synergies, the model considers the complete set of the airports $\mathcal{N}$ and only restricts the set of airports as candidates for charging bases; (2) add a constraint to force z^* (which is given by the incumbent optimal objective value) be a valid lower bound of the restricted problem. If a feasible solution to the restricted problem is found, we add the activated airports $\mathcal{A}$ to the kernel, update the incumbent objective value z^* and store the solution. The currently best found solution is used to warm start the solution process. After we assess all buckets, we increment the iteration count. If the iteration count is less than or equal to $iter^{\max}$ (and the run-time of the algorithm $runtime$ is less than or equal $T^{\max}$), we start the next iteration, which begins with re-building the buckets from the remaining airports outside the kernel. Note that having two termination criteria is helpful, since one iteration involves solving $|\mathcal{B}|$ optimization problems, which may be time consuming.

Algorithm 1 EACN-KS algorithm.

Input: all airports $\mathcal{N}$; maximum iterations $iter^{\max}$; kernel size $\bar{s}$; bucket size $\bar{b}$; maximum run time $T^{\max}$

Initialization:
  Build the initial kernel: $\mathcal{S} = INIT(\mathcal{N}, \mathcal{P}, \mathcal{K}, \bar{s})$
  Iteration count: $iter \leftarrow 0$
  Objective value: $z^* \leftarrow 0$
while $iter \leq iter^{\max}$ and $runtime \leq T^{\max}$ **do**
  Create set of non-kernel airports: $\mathcal{U} \leftarrow \mathcal{N} \setminus \mathcal{S}$
  Create set of buckets $\mathcal{B} \leftarrow \emptyset$
  while $\mathcal{U}$ is not empty **do**
    Randomly pick $\bar{b}$ airports from $\mathcal{U}$ and add to a bucket b
    Add bucket to the set of buckets: $\mathcal{B} \leftarrow \mathcal{B} \cup b$
    Remove bucket airports from $\mathcal{U}$: $\mathcal{U} \leftarrow \mathcal{U} \setminus b$
  end while
  for $b \in \mathcal{B}$ **do**
    Solve restricted model: $EACN^*(\mathcal{S} \cup b, z^*)$
    if $EACN^*(\mathcal{S} \cup b, z^*)$ is feasible **then**
      Get activated airports: $\mathcal{A} = \{i \in \mathcal{S} \cup b : y_i = 1\}$
      Update the kernel: $\mathcal{S} \leftarrow \mathcal{S} \cup \mathcal{A}$
      Update the objective value: z^*
      Store solution (z^*, y_i, ρ_i, z_{ij}, ϕ_p, ψ_k^d).
    end if
  end for
  Update iteration count: $iter \leftarrow iter + 1$
end while

Output: z^*, y_i, ρ_i, $z_{i,j}$, ϕ_p, ψ_k^d

4. Computational experiments

In this section, we examine the computational tractability of the EACN-REG and test the performance of our proposed Kernel Search based algorithm (EACN-KS) using randomly generated networks of varying size and complexity.

The size of our instances is controlled by the number of candidate airports $|\mathcal{N}|$, the number of population areas $|\mathcal{K}|$, and the maximum travel range on a single charge τ. All together, they affect the computational complexity of the model. Specifically, the number of airports significantly impacts the solution space by linearly increasing the number of candidates for locating charging bases and exponentially increasing the number of potential paths. The number of feasible paths is also significantly affected by τ, as longer values render more edges between airports feasible, which in turn results in more travel path options. Ultimately, the number of population areas directly affects the complexity of achieving connectivity targets.

We consider a geographic bounding box (area) with a total area of 450,000 square kilometers, comparable with the geographical

span of Sweden. Then, we partition the bounding box using grids of various sizes, either 100 (4500 square kilometers per area) or 200 (2250 square kilometers per area) to obtain the population areas, and randomly select one of the grid cells as a target destination. We randomly generate 50 or 100 airports within the bounding box, ensuring that any pair of airports is at least 30 kilometers apart. Notice that these airport networks are reasonable representations of the real-world; for example, an airport network size of 50 represents the active (with scheduled traffic) airports in several countries (e.g., ≈ 47 in Norway, ≈ 39 in Sweden, and ≈ 40 in Italy), while 100 suitably proxies the possible network size if currently active airports are coupled with currently underutilized airfields/regional airports that could be leveraged for the operations of electric aircraft (68 in Norway, 83 in Sweden, 116 in Italy) (Our Airports, 2021). For the maximum aircraft range, we examine instances with three values of τ (400, 600, and 800) based on the information reported by electric aircraft manufacturers (e.g., Eviation, 2021; Heart Aerospace, 2021) and prior studies (e.g., Justin et al., 2022).

Given the airport network, we calculate the flight distance between airport pairs as the geodesic distance and consider a cruise speed of 400 kilometer per hours to calculate the corresponding flight times. We then use a simple-paths algorithm based on a modified depth-first search (Hagberg et al., 2008; Sedgewick, 2001), to generate all the potential paths from any airport to the target destination with a maximum of two intermediate airports (i.e., maximum of three adjacent edges). Note that the performance of this algorithm was sufficiently good for the real-world like cases considered, taking about 5 minutes for the largest instances that are also representative of real world cases.[10] Consistent with previous literature (e.g., Paleari et al., 2010), we remove unattractive paths for a given origin airport by enforcing a maximum threshold on the routing factor—calculated as the ratio between the path's total flight distance and the nonstop flight distance between the origin and destination airport—equal to 1.4 when $\tau = 400$ and 1.2 when $\tau = 600/800$. We compute ground access times by dividing the geodesic distance between the centroid of each grid cell and each airport by an average speed of 60 kilometer per hours and restrict to paths whose origin airport is within 90 minutes driving time from the grid cell centroid.

Overall, we consider 12 scenarios and run 5 instances for each, leading to a total of 60 instances, which are solved by branch-and-cut (B&C) with our tightened formulation and the EACN-KS heuristic proposed in Section 3. Due to a lack of data, in our computational experiments and the following application in Section 5, we do not differentiate between airports (i.e., we assume $c_i = 1, \ \forall i \in \mathcal{N}$) and assume no explicit cost associated with the use of airports not considered as charging bases. Yet, the model could be trivially extended to account for these aspects. For the B&C, we solve the two objectives of the model lexicographically: we first solve for the coverage objective, store the value of the (optimal) coverage and then solve for the minimum number of airports with charging infrastructure while enforcing the value of the total coverage as a constraint. For the KS, we consider weights $\mu_1 = 1$ and $\mu_2 = 0.01$, which ensure the prioritization of the first objective (coverage) versus the second one (number of charging bases).[11] Note that, solving the problem lexicographically eases the comparison among methods from the computational point of view as it returns one optimal solution for each instance (instead of a Pareto front). Prioritizing the coverage is also significant from a practical point of view as it constitutes a typical planning goal of regional transportation planners, especially in the case of ensuring regional connectivity. The sizes of the initial kernel and the buckets—equal to 5 and 10, respectively—were determined through experimentation. The kernel search algorithm was implemented using Python 3.6 and the CPLEX MILP Solver (v12.9), on an Intel(R) Core(TM) i7-8700K CPU with a frequency of 3.70 gigahertz and 32 gigabyte of RAM, enforcing a maximum run-time of 20 minutes and 2 hours for each individual MILP and the overall algorithm, respectively.

Table 2 summarizes the results of the computational experiments. For each scenario defined by $|\mathcal{N}|$, $|\mathcal{K}|$ and τ, the table reports the instance number (#), the number of variables (# cols) and constraints (# rows), and the coverage value (Obj_1) (assuming equal weights for each population area), the number of airports selected as charging bases (Obj_2) and the computational time in seconds (T(s)). For the B&C, the Lower bound (LB) of the number of airports selected as charging bases is reported to indicate the optimality gap. For the KS, we report the results for two different implementations, where the first one (EACN-KS(1)) is limited to one iteration while the second one (EACN-KS) considers a maximum of three iterations. Observing the differences between them highlights the benefits of reiterating among and recombining buckets. For the KS methods, the table also reports the percentage difference (Δ%) in their coverage and number of charging bases as compared to the B&C approach.

The computational results reveal that the B&C approach can efficiently solve small to medium sized instances to optimality, such as instances with 50 airports within 9 minutes. By contrast to when the problem size is increased to 100 airports, the B&C approach suffers from scalability issues thus attaining feasible but most often sub-optimal solutions within the two hours threshold. The B&C approach especially struggles with larger instances that consider long ranges of 600 kilometers, and even more for 800 kilometers, which lead to a significant enlargement of the solution space ($\approx$2 to 4 times in the number of rows and cols). Despite the strengthening of the model formulation, a closer look into the convergence of the B&C algorithm reveals a critical issue with the loose LP relaxation of the EACN-REG—for example, in the largest instances with $\tau = 800$ (instances 41 to 45 and 56 to 59), the lower bound on the number of charging bases is still equal to 0 after two hours—which in turn undermines the effectiveness and convergence of tree-based enumeration algorithms.

Now let us turn to our KS heuristic. For small-mid size instances (instances 1 to 30), our experiments reveal that using one iteration through the buckets is not sufficient to consistently achieve global optimality. The EACN-KS(1) reports sub-optimal results for the coverage objective in 7 out of 30 instances, with an optimality gap ranging between -2% and -20%. Additionally, even when EACN-KS(1) gets the coverage objective right, there are some instances (e.g., instances 5, 8, 16, and 19) in which it does not achieve the optimum concerning the number of airports activated as charging bases. This, in turn, highlights the limitation of performing only one iteration through the set of pre-assembled buckets, as it may fail to capture some correlation patterns among airports, ultimately yielding sub-optimal results. By contrast, when considering larger instances (instances 31 to 60), EACN-KS(1) appears to have a significant edge against B&C. In these instances, the EACN-KS(1) attains optimal coverage[12] in all the instances but four (instances 33, 47, 49, and 50), and reduces the number of bases

[10] Furthermore, note that in case the enumeration of path would be problematic, our set partitioning approach is anyhow amenable to the implementation of column generation like heuristics or exact branch and price algorithms (similar to Barnhart et al., 1998a; 1998b).

[11] Solving lexicographically for the Kernel Search is not viable as enforcing a coverage constraint would lead to in-feasibility in the first steps of the algorithm (i.e., exploration of the first set of buckets). Additionally, solving B&C sequentially or with weights neither affected the computational performance nor the optimal objective.

[12] Recall that, under the B&C approach, we are solving the problem sequentially—first maximizing coverage and then minimizing the number of charging bases under a maximum coverage constraint. The first step is trivial and solves in a matter of

Table 2
Computational experiments.

#	$\|\mathcal{N}\|$	$\|\mathcal{K}\|$	τ	B&C					EACN-KS(1)			EACN-KS		
				#cols	#rows	Obj_1	Obj_2(LB)	T(seconds)	Obj_1(Δ%)	Obj_2(Δ%)	T(seconds)	Obj_1(Δ%)	Obj_2(Δ%)	T(seconds)
1	50	100	400	2367	8077	100	14 (14)*	≤ 60	98 (−2%)	13 (−7%)	≤ 60	100 (=)	14 (=)	≤ 60
2				2613	8936	100	15 (15)*	≤ 60	97 (−3%)	14 (−7%)	≤ 60	100 (=)	15 (=)	≤ 60
3				2293	7736	92	16 (16)*	≤ 60	74 (−20%)	13 (−19%)	≤ 60	92 (=)	16 (=)	≤ 60
4				1889	6362	68	14 (14)	≤ 60	68 (=)	14 (=)	≤ 60	68 (=)	14 (=)	≤ 60
5				2388	8172	93	17 (17)*	≤ 60	90 (−3%)	16 (−6%)	≤ 60	93 (=)	17 (=)	≤ 60
6	50	100	600	3558	12,172	100	9 (9)*	225	100 (=)	9 (=)	≤ 60	100 (=)	9 (=)	≤ 60
7				4717	16,869	100	7 (7)*	98	100 (=)	8 (+14%)	≤ 60	100 (=)	7 (=)	80
8				5029	17,907	99	8 (8)*	109	99 (=)	9 (+13%)	≤ 60	99 (=)	8 (=)	230
9				3637	12,662	98	8 (8)*	≤ 60	98 (=)	8 (=)	≤ 60	98 (=)	8 (=)	≤ 60
10				4207	14,804	100	8 (8)*	≤ 60	100 (=)	8 (=)	≤ 60	100 (=)	8 (=)	≤ 60
11	50	100	800	7762	28,399	98	4 (4)*	486	98 (=)	4 (=)	≤ 60	98 (=)	4 (=)	296
12				8078	29,642	100	5 (5)*	323	100 (=)	5 (=)	≤ 60	100 (=)	5 (=)	388
13				6451	23,087	97	4 (4)*	127	97 (=)	4 (=)	≤ 60	97 (=)	4 (=)	116
14				5720	19,977	98	4 (4)*	65	98 (=)	4 (=)	≤ 60	98 (=)	4 (=)	171
15				5304	18,473	100	4 (4)*	92	100 (=)	4 (=)	≤ 60	100 (=)	4 (=)	114
16	50	200	400	2314	7794	116	14 (14)*	≤ 60	106 (−9%)	11 (−21%)	≤ 60	116 (=)	14 (=)	≤ 60
17				2581	8668	198	20 (20)*	≤ 60	198 (=)	20 (=)	≤ 60	198 (=)	20 (=)	≤ 60
18				2496	8426	180	17 (17)*	≤ 60	172 (−4%)	17 (=)	≤ 60	180 (=)	17 (=)	≤ 60
19				2494	8291	192	20 (20)*	≤ 60	181 (−6%)	16 (−20%)	≤ 60	192 (=)	20 (=)	≤ 60
20				2932	10,084	144	13 (13)*	≤ 60	144 (=)	13 (=)	≤ 60	144 (=)	13 (=)	≤ 60
21	50	200	600	4387	15,224	190	7 (7)*	83	190 (=)	7 (=)	≤ 60	190 (=)	7 (=)	≤ 60
22				4183	14,391	196	8 (8)*	139	196 (=)	8 (=)	≤ 60	196 (=)	8 (=)	≤ 60
23				5156	18,032	198	8 (8)*	168	198 (=)	8 (=)	≤ 60	198 (=)	8 (=)	≤ 60
24				5595	19,899	200	9 (9)*	≤ 60	200 (=)	9 (=)	≤ 60	200 (=)	9 (=)	≤ 60
25				5517	19,689	198	8 (8)*	≤ 60	198 (=)	8 (=)	≤ 60	198 (=)	8 (=)	≤ 60
26	50	200	800	6126	21,348	193	4 (4)*	292	193 (=)	5 (+25%)	116	193 (=)	4 (=)	484
27				8264	29,956	200	5 (5)*	248	200 (=)	5 (=)	≤ 60	200 (=)	5 (=)	326
28				6452	22,943	193	4 (4)*	337	193 (=)	5 (+25%)	≤ 60	193 (=)	5 (+25%)	379
29				5674	19,595	197	4 (4)*	129	197 (=)	4 (=)	≤ 60	197 (=)	4 (=)	220
30				5146	17,767	198	5 (5)*	90	198 (=)	6 (+20%)	≤ 60	198 (=)	5 (=)	275
31	100	100	400	12,595	46,162	98	20 (13)	TL	98 (=)	18 (−10%)	80	98 (=)	17 (−15%)	4222
32				12,837	47,038	98	18 (14)	TL	98 (=)	17 (−6%)	102	98 (=)	17 (−6%)	2394
33				13,996	51,627	100	18 (12)	TL	94 (−6%)	16 (−11%)	75	100 (=)	16 (−11%)	1871
34				13,175	48,466	98	17 (14)	TL	98 (=)	17 (=)	≤ 60	98 (=)	16 (−6%)	158
35				13,124	48,207	100	19 (19)*	1571	100 (=)	19 (=)	69	100 (=)	19 (=)	1024
36	100	100	600	25,278	94,053	100	12 (1)	TL	100 (=)	7 (−42%)	281	100 (=)	6 (−50%)	1675
37				30,368	114,252	97	12 (4)	TL	97 (=)	9 (−25%)	287	97 (=)	9 (−25%)	1411
38				24,931	92,972	99	11 (4)	TL	99 (=)	10 (−9%)	129	99 (=)	8 (−27%)	3239
39				22,990	85,132	99	11 (3)	TL	99 (=)	8 (−27%)	453	99 (=)	8 (−27%)	TL
40				29,505	110,991	98	14 (3)	TL	98 (=)	8 (−43%)	194	98 (=)	8 (−43%)	1621
41	100	100	800	46,847	178,389	99	8 (0)	TL	99 (=)	5 (−38%)	TL	99 (=)	5 (−38%)	TL
42				46,360	176,225	96	6 (0)	TL	96 (=)	5 (−17%)	4866	96 (=)	5 (−17%)	TL
43				23,881	86,140	99	6 (0)	TL	99 (=)	4 (−33%)	6105	99 (=)	4 (−33%)	TL
44				38,486	144,236	98	8 (0)	TL	98 (=)	5 (−38%)	TL	98 (=)	5 (−38%)	TL
45				49,094	186,039	98	11 (0)	TL	98 (=)	5 (−55%)	TL	98 (=)	5 (−55%)	TL
46	100	200	400	15,008	55,087	196	18 (12)	TL	196 (=)	18 (=)	139	196 (=)	17 (−6%)	2340
47				11,498	41,431	190	22 (22)*	3640	181 (−5%)	21 (−5%)	≤ 60	190 (=)	22 (=)	375
48				13,257	48,398	196	18 (13)	TL	196 (=)	18 (=)	94	196 (=)	17 (−6%)	2066
49				9107	32,149	176	21 (21)*	84	162 (−8%)	18 (−14%)	≤ 60	176 (=)	21 (=)	115
50				12,025	43,502	157	21 (21)*	141	147 (−6%)	19 (−10%)	≤ 60	157 (=)	21 (=)	181
51	100	200	600	26,197	97,004	195	13 (1)	TL	195 (=)	8 (−38%)	256	195 (=)	7 (−46%)	1651
52				22,449	82,062	199	9 (0)	TL	199 (=)	7 (−22%)	1368	199 (=)	7 (−22%)	TL
53				19,525	70,999	199	9 (1)	TL	199 (=)	8 (−11%)	535	199 (=)	8 (−11%)	5295
54				15,811	56,244	195	10 (2)	TL	195 (=)	9 (−10%)	1769	195 (=)	9 (−10%)	TL
55				16,932	60,359	191	8 (2)	TL	191 (=)	8 (=)	427	191 (=)	8 (=)	3703
56	100	200	800	28,493	104,449	196	6 (0)	TL	196 (=)	5 (−17%)	TL	196 (=)	5 (−17%)	TL
57				30,110	111,218	198	5 (0)	TL	198 (=)	5 (=)	5369	198 (=)	4 (−20%)	TL
58				20,186	71,517	197	6 (0)	TL	197 (=)	4 (−33%)	4324	197 (=)	4 (−33%)	TL
59				211,474	55,358	200	7 (0)	TL	200 (=)	5 (−29%)	4115	200 (=)	5 (−29%)	TL
60				84,024	23,559	198	5 (1)	TL	198 (=)	4 (−20%)	2952	198 (=)	4 (−20%)	TL

Obj_1 stands for the coverage objective (with equal weights and one target destination), i.e., $\sum_{k\in\mathcal{K}} \phi_k$; Obj_2 stands for the number of airports activated as charging bases, i.e., $\sum_{i\in\mathcal{N}} y_i$; Δ% computed w.r.t B&C solution; Asterisks (*) denote global optimal solutions; TL denotes the maximum run-time of two hours.

significantly (by 26.2%, on average[13]). This highlights the benefits of the KS in coping with large instances.

Next we show how leveraging more iterations and recombination of buckets in the Kernel search achieves a trade-off between solution quality and computational times, outperforming both B&C and EACN-KS(1). Overall, EACN-KS achieves optimal coverage across all scenarios and instances, and returns the smallest number of charging bases in all of the instances but one (instance 28). For small- and mid-size instances (e.g., instances 1 to 30), EACN-KS consistently finds the global optimal solution in short computation times—overcoming the limits of considering one iteration only and matching the performance of B&C. More inter-

seconds. Hence, the coverage level reported under B&C is always optimal. In turn, this helps assess the quality of our heuristic solution.

[13] Considering instances for which coverage is optimal under both methods.

estingly, the KS achieves superior solutions for the large instances (i.e., instances 31 to 60), with a significant percentage reduction in the number of charging bases of −24.4% and −5.2% on average as compared to B&C and EACN-KS(1), respectively. In our instances, a closer look into the evolution of the algorithm highlights that at termination, the kernel size ranges between 12 and 58. These figures provide information about the maximum size of MILP subproblems considered in the Kernel Search because the kernel size is non-decreasing, i.e., we do not remove items from the kernel. In turn, this highlights the ability of EACN-KS to effectively decompose the large-scale original EACN-REG into a series of subproblems of reduced size, with clear benefits in terms of computational tractability.

In summary, these computational results show that the B&C approach is not suitable for solving instances of reasonable size: its performance drastically worsens as the number of candidate airports, as well as the range on a single charge, increases. By contrast, the results highlight consistent and strong performance of the proposed KS approach, ultimately providing an effective and scalable solution method for the EACN-REG model.

5. Case study

The application of the EACN-REG is now illustrated through a case study of Sweden—one of the leaders in the transition towards electric aircraft. The Swedish government, through the Swedish Transport Administration (Trafikverket), is interested in ensuring good connectivity for all regions to/from certain major destinations, such as a major city or a hub airport, to foster regional cohesion and development (Andersson, 2019). Trafikverket analyses the travel opportunities of all regions to certain destination(s) and makes infrastructure recommendations to maximize regional connectivity. The deployment of electric aircraft is a major opportunity for improving regional connectivity. Specifically, their small seat capacity and lower operating costs can effectively serve regional routes, including those with thin demand serving remote regions, which do not have good connectivity either with ground transportation or commercial airline services due to insufficient passenger demand. These remote regions typically rely on high public subsidies to have air services (Kinene et al., 2022).

Through this case study, we highlight the strategic planning insights that the EACN-REG model can provide concerning the structuring of a charging network for electric aircraft and the associated connectivity implications.

As input to our real-world case study, we divided Sweden into 281 (50 kilometers by 50 kilometers) population areas. Each population cell has an associated population that we obtained from a high-resolution (30 arcseconds) global spatial data set for 2019, similar to Tatem (2017). Concerning the set of airport candidates, we consider two alternative settings. In Sweden, electric aircraft can utilize the current network of 38 airports—that we refer to as the *current network*—already with air traffic management and instruments (e.g., lighting and technical equipment) to operate commercial traffic. Moreover, we show how regional connectivity can expand by leveraging a larger network of 83 airports—that we refer to as the *full network*—consisting of 45 underutilized airports with at least one 800 meters long paved runway (TrafikAnalys, 2020). In line with current aircraft operation requirements (see ICAO, 2021), we account for alternate airport requirements and contingency energy by adjusting the definition of arc flight distance parameters in the model formulation. First, we account for diversions to an alternate airport by estimating the distance to the airport closest to the flights destination (alt_j). In our case, the *current network* gives the minimum, median, and maximum distances to alternate airports of 33, 77 and 159 kilometers, respectively, while *full network* gives 8, 38 and 154 kilometers, respectively. Second, we account for the additional en-route energy consumption caused by wind, routing changes or air traffic management restrictions—also known as flight reserve/contingency energy—by increasing the flights distance by a factor (res) equal to 5%. We thus define an adjusted distance of each flight arc in our model as follows: $\hat{d_{ij}} = d_{ij} * (1 + res) + alt_j$. To assess regional connectivity, we consider one target destination, Stockholm city—which is commonly used when assessing regional connectivity in Sweden (see, e.g., Kinene et al., 2022). The total travel time between the centroids of the population areas and Stockholm using a given path was then computed as the sum of ground access and flight times following a similar approach as in the computational experiments (Section 4).[14] Finally, we apply the following filtering to the input data, based on current practice and commonly used criteria in air transportation research. In addition to the thresholds on the routing factor and ground access time as in Section 4, we consider a total travel time threshold (e.g., 4 hours) to account for connectivity targets stated by transportation authorities. In practice, for each population area, we consider those flight paths that, when combined with the ground access component, provide a total travel time within a given travel time threshold. Ultimately, we consider only population outside of the Stockholm area. We assume that the areas with 2 hours of ground transportation to Stockholm city already have sufficient connectivity, and it would be unattractive for them to drive to a nearby airport for a flight to Stockholm.

Given the data input specific to Sweden, we conduct a two-part analysis to (i) investigate the trade-off between population and regional coverage and number of charging bases and (ii) assess the impact of technological (and safety) features of electric aircraft, specifically the maximum range on a single charge (τ), and the total travel time threshold. All results in the case-study were obtained by solving the EACN-REG with our kernel search heuristic—with the same computer and run-time limits as in the computational experiments in Section 4.

5.1. Coverage and number of charging bases

In Fig. 2, we present the Pareto front curves of the coverage (on the y-axis) and the number of charging bases (on the x-axis) for the *current network* (Curr. Ntw) and the *full network* (Full. Ntw). The Pareto fronts are obtained by an approach similar to the ϵ-constrained method, i.e, by maximizing the coverage objective (Eq. (1)), subject to a constraint on the number of charging bases (Eq. (2)). We also investigate two alternative regional connectivity targets, i.e., either maximizing the spatial coverage (i.e., unweighted regional coverage, proxied by the number of covered cells) or maximizing population coverage.[15] Fig. 2(a) and (b) report the results under spatial coverage maximization; while Fig. 2(c) and (d) refer to population coverage maximization. Notice that the irregular patterns in Fig. 2(b) and (c) are due to the fact that we optimize for one objective and then assess the solution based on the other objective. This in turn highlights the degree of correlation/divergence between objectives—underscoring the importance to carefully set the connectivity requirements. All analyses consid-

[14] We acknowledge the fact that these inputs could be refined. For example, ground access travel times could be obtained from well known journey planning search engines, such as google maps and Rome2Rio, similar to Birolini et al. (2019). Similarly, the estimation of flight times could be improved by explicitly accounting for take-off and landing, or considering transfer time between connecting flights. While this may surely improve the practical insights and reliability of the analysis from an empirical standpoint, it does not significantly affect the illustration of the EACN-REG's applicability and strategic insights from a modeling standpoint, which is the primary aim of this paper.

[15] Practically, these two approaches are implemented by varying input parameter π_k, setting it equal to 1 in the former case and equal to the population living in k in the latter case.

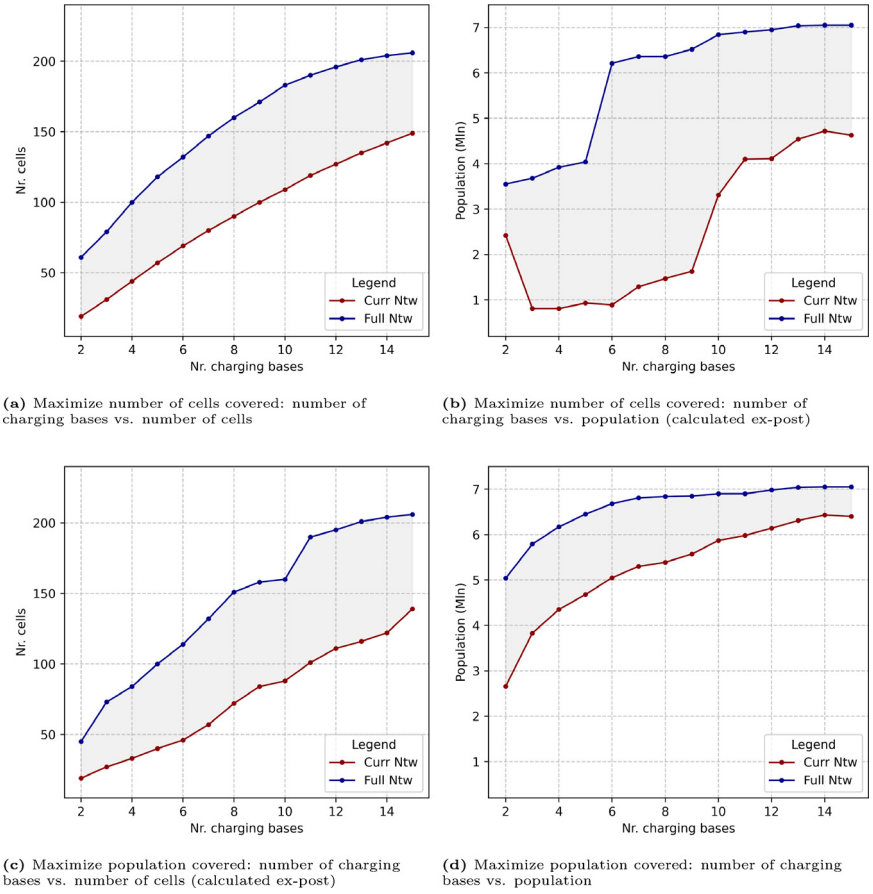

(a) Maximize number of cells covered: number of charging bases vs. number of cells

(b) Maximize number of cells covered: number of charging bases vs. population (calculated ex-post)

(c) Maximize population covered: number of charging bases vs. number of cells (calculated ex-post)

(d) Maximize population covered: number of charging bases vs. population

Fig. 2. The trade-off between coverage (Nr. cells or population) and number of charging bases (Nr. Charging bases).

ered a maximum range on a single charge of 400 kilometers and a total travel time threshold of 4 hours.

As expected, Fig. 2 shows that having more airports as charging bases enables the coverage of more areas and population. Moreover, the pattern is non-decreasing downward concave, showing how with a small number of airports (e.g., 10) we can serve the majority of cells/population, while it takes an increasing number of airports to achieve maximum coverage, including remote regions. This is also evident from the maps in Fig. 3. This is especially true in a population weighted (Fig. 2(d)) rather than unweighted approach (Fig. 2(a)), further highlighting the difficulty of serving remote regions. We also notice that leveraging a *full network* of airports (blue line), which includes the underutilized regional airports/airfields, has two main benefits. First, it allows to reduce the number of charging bases but achieve the same level of coverage, e.g., 4 vs. 9 airports to get the same coverage in terms of number of cells (Fig. 2(a)), and 2 vs. 6 (Fig. 2(d)) to get the same coverage in terms of population. Second, it can achieve more coverage/connectivity than the *current network* of airports (red line): for example, with the *current network*, locating charging bases at 9 airports would provide coverage for 5.57 million people (and 84 population areas) but if the *full network* is leveraged, 15.7% more people (and 19.1% more population areas)—totaling 6.45 million people—would have coverage but with 5 (44.4% less) airports. Overall, these results show how leveraging a more widespread network of airports can boost connectivity, both in terms of efficiency and scope.

Comparing Fig. 2(b) and (d), clearly illustrates that ensuring spatial coverage of areas based on uniform weights is not fully correlated with maximizing the population covered. This, in turn, highlights the flexibility of the EACN-REG model to accommodate and assess the outcome of different planning priorities.

Fig. 3 then highlights the incremental coverage of population areas with the increase in the number of airports activated as charging bases. In Fig. 3(a), it can be seen that locating a charging base at only three airports (i.e., Norrköping, Gävle-Sandviken, and Anderstorp) can provide coverage to 73 areas and 5.8 million people (i.e., 81.9% of maximum coverage) in the south and central part of Sweden—the most densely populated area other than Stockholm. With 6 airports as in Fig. 3(b), 6.7 million people and 56.2% more areas would be covered. Then, with 9 airports as charging bases (Fig. 3(c)), we could achieve almost full coverage, except remote areas specifically in the north (e.g., in Kiruna) and Gotland—Sweden's large island—with 211,000 people (3.0% of the population). These areas would require two additional charging bases: for example, one at Gällivare airport to increase coverage in the north and another either on Gotland (i.e, at Visby airport). Overall, this analysis demonstrates that the full benefits of electric aircraft can better be achieved by leveraging the many currently under-utilized regional airports. Additionally, using the population as a measure of geographic importance for the population areas allows to achieve better trade-off between the population covered and the number of charging bases than using equal weights of geographic importance. Yet, this may be against a more equitable coverage of areas, at the expense of remote regions.

5.2. Travel time threshold and maximum aircraft range

In this part, we assess how the different maximum ranges and the consideration of different travel time thresholds would af-

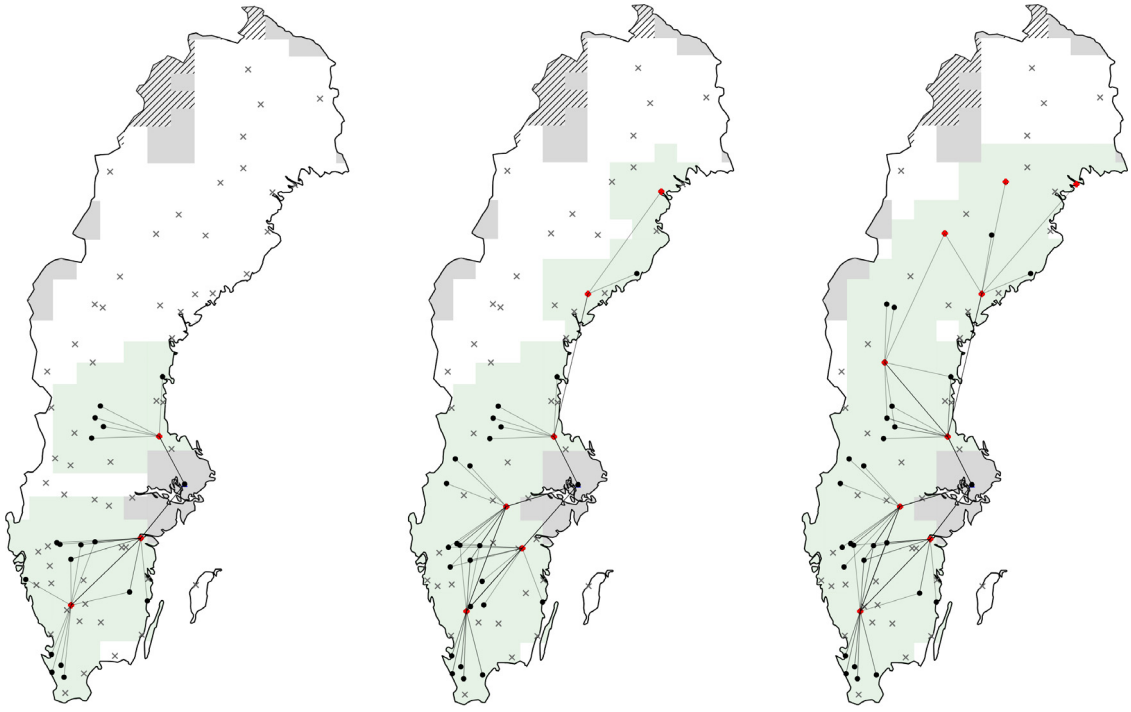

(a) 3 airport (b) 6 airports. (c) 9 airports.

Fig. 3. The location of the airports selected as charging bases and the covered population areas—using the full network of candidate airports under a population coverage maximization approach. The white area represents uncovered population areas; gray area represents the Stockholm area and those unreachable areas based on the considered empirical setting; hatched area represents population areas with zero population; light-green area represents covered population areas; red dots represent the airports activated as charging bases; black dots represent the other airports used; gray crosses represent unused airports; and solid black lines indicate edges along selected paths. (For interpretation of the references to color in this figure legend, the reader is referred to the web version of this article.)

Table 3
The impact of the total travel time threshold and maximum range on a single charge τ on the coverage, number of airports selected as charging bases, and mean and standard deviation of the minimum total travel times of selected paths across all origins.

TTT	$^*\tau$	Curr. network					Full. network				
		Cov Pop	Cov Nr.cells	Nr.Chg Apts	TTT Mean	TTT Std	Cov Pop	Cov Nr.cells	Nr.Chg Apts	TTT Mean	TTT Std
180	400	6.62	165	24	113.9	31.9	7.02	193	19	109.2	33.5
	600	6.67	183	13	115.8	34.1	7.05	203	10	105.6	38.1
	800	6.67	183	6	115.2	34.5	7.05	204	10	103.1	37.8
240	400	6.64	173	23	118.2	35.6	7.06	207	16	117.2	40.3
	600	6.70	211	13	126.6	43.2	7.07	227	11	115.8	46.9
	800	6.70	211	5	127.3	44.2	7.07	227	11	113.0	46.5
300	400	6.64	173	23	118.2	35.6	7.06	207	16	117.2	40.2
	600	6.70	211	13	127.9	44.8	7.07	227	11	115.7	46.9
	800	6.70	211	5	127.3	44.2	7.07	227	10	113.1	46.7

fect the coverage, number of airports activated as charging bases, and travel-times from each origin to the destination. We explore three total travel time thresholds—3, 4 and 5 hours—and three values of the maximum range on a single charge τ—400, 600, and 800 kilometers. These values of τ are both in line with the published values by promising aircraft manufacturers (Eviation, 2021; Heart Aerospace, 2021) and literature (e.g., Justin et al., 2022).[16] The results are shown in Table 3 and Fig. 4. Table 3 presents, for each airport network (i.e., *current network* and *full network*) and each combination of total travel time thresholds (TTT) and τ, the covered population (Cov Pop) and number of areas (Cov Nr.cells), number of airports selected as charging bases (Nr.Chg Apt), and the mean (TTT Mean) and standard deviation (TTT Std) of the minimum total travel times across all origins—computed considering the most convenient viable path from each origin. Fig. 4 presents the total travel times (on the y-axis) of all feasible paths of each served origin (on the x-axis) for two airport networks.

First, let us discuss the impact of varying the total travel time threshold. Increasing the total travel time threshold would allow the coverage of more areas and population, with less airports selected as charging bases. We notice that above a certain travel time threshold (4 hours for the case of Sweden), no improvement in coverage would be achieved (regardless of the range). In turn, neither the current nor the full network of candidate airports would be sufficient to cover a set of very remote regions (i.e., the gray areas other than Stockholm depicted in Fig. 3): this would only be possible by either increasing the access time threshold (i.e., more

[16] We also conducted additional analyses to test a lower viable maximum aircraft range of 300 kilometers as a means to account for more stringent safety concerns (e.g., than with 400 kilometers), but the EACN-REG was infeasible for our specific case study.

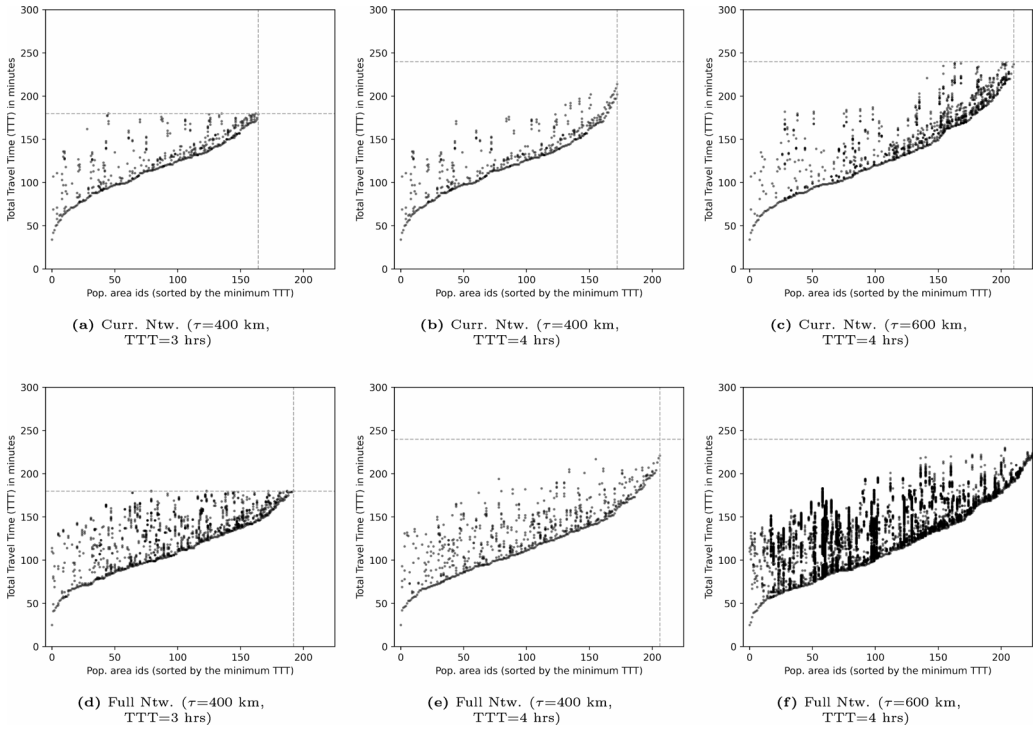

Fig. 4. The total travel times of all selected paths of each served origin when considering the two airport networks *current network* (Curr. Ntw.) and *full network* (Full Ntw.), a maximum travel range τ (i.e., 400 and 600 kilometers), two total travel time thresholds TTT (i.e., 3 and 4 hours). Each black dot represents a possible path for an origin.

than 90 minutes) or considering the establishment of new airport candidates. From Table 3, considering the *full network (current network)*, an increase in the total travel time threshold by 1 hour allows coverage of 0.4% (0.3%) more population and 10.1% (11.8%) more areas but with fewer airports. Indeed, a higher total travel time threshold allows for the coverage of more people (and areas), especially those furthest from the destination, by allowing the use of additional paths with longer travel times. This increase in coverage, the number of paths, and the minimum total travel time across origins is presented in more detail using Fig. 4. For example, with the *current network* and a range of 400 kilometers, a total travel time threshold of 4 hours in Fig. 4(b), compared to 3 hours in Fig. 4(a), covers more areas (indicated by the right-shift dotted vertical line), which use additional paths with the longer travel times—indicated by the increase in the number of dots above 3 hours). Indeed, a similar comparison for the *full network* (Fig. 4(d) and (e)) shows the same pattern but with higher coverage and more possible paths for each area.

Moving now to the investigation of the impact of the maximum aircraft range, we observe from Table 3 that increasing it from 400 to 600 kilometers requires the use of less charging bases (ranging −31%−−47%) to achieve slightly more coverage (ca. 1%) for a given travel time threshold. On the other hand, we notice that a range higher than 600 kilometers (e.g., 800 kilometers) does not significantly improve the coverage. Additionally, an increase in the range is found to have remarkable connectivity benefits. First, it will reduce the minimum total travel time across origins by making more direct paths possible. Second, it increases the number of viable paths, thus giving more flexibility to later planning stages concerning flight scheduling and fleet assignment. This latter aspect is evident from a comparison of Fig. 4(e) and (f) by the significant increase in the number of dots).

Lastly, considering the average changes in coverage and TTT Mean between the *current network* and the *full network* across the nine scenarios in Table 3 suggests that leveraging the many currently under-utilized regional airports has connectivity and investment benefits (on average +12.1% in number of regions covered, +5.8% in population coverage and −7.3% reduction of travel times).

These analyses have elaborated the trade-off between various design aspects to be considered when strategically planning for the adoption of electric aircraft. As the results have shown, the proposed EACN-REG model can provide effective decision support to policymakers and transportation/regional planners in this task.

6. Conclusions

Following the recent technological advancements and growing attention towards sustainability, electric aviation appears today as an effective and concrete means to decarbonize aviation. Yet, the wide-scope adoption of electric aircraft cannot happen without proper supporting infrastructures, which in turn need to be planned upfront even with limited traffic in the early years.

This paper contributes to these efforts by developing a novel optimization model—referred to as *Electric Aircraft Charging Network for Regional Routes (EACN-REG)*—to support the strategic planning of electric aircraft charging networks in a regional context. The EACN-REG defines the network of airports and flight paths to optimally trade-off the number of charging bases (and associated investment costs) with connectivity and population coverage targets.

From a technical standpoint, the EACN-REG is formulated as a multi-objective uncapacitated facility location problem, with additional complexities due to the short range and multi-step operations of electric aircraft, which make it very difficult to solve. Hence, we have developed a tailored Kernel Search heuristic—which effectively scales to large instances by decomposing the problem in a series of MILP of reduced size. Computational experiments using real-world-like randomly generated instances have demonstrated the greater performance of our heuristic method compared to exact branch-and-cut algorithms, being able to consistently achieve near-optimal solutions in shorter computational time for all the instances considered.

An extensive real-world case study of Sweden has highlighted the practical insights that can be derived from the application of the EACN-REG model. Results have shown how the model can effectively inform planners and policymakers, highlighting the benefits of considering an extensive set of airport candidates as a key advantage of small electric aircraft, and testing the implications of range increases and total travel time thresholds. We acknowledge that, although we obtained the range inputs from reliable official sources published by aircraft manufacturers, the actual ranges are subject to some level of uncertainty especially regarding developments in battery technology. Nevertheless, the proposed methodology provides valid methodological foundations to investigate this uncertainty (e.g., by testing various scenarios) and assess the impact of ranges to the connectivity provided by this new technology.

In conclusion, the EACN-REG provides a valid foundation for future modeling efforts in the area of electric aircraft network planning. However, there are plenty of opportunities for continuing research in the area. First, future research efforts could be devoted to integrating the strategic perspective of the EACN-REG with more tactical and operational decisions. This would require suitable methods to estimate demand in thin markets as a key input to support the sizing and operations of both aircraft fleets and charging facilities. Second, an interesting direction for future research is to delve further into the cost of operating the charging facilities and the aircraft, and explore how this might impact the optimal trade-off with regional connectivity and the overall system cost and design. Note that accurate assessment of these costs would require consideration of tactical aspects such as aircraft flight schedules: this may be addressed with a two-stage modeling framework and also require more detailed (not yet known) inputs on electric aircraft operations. Third, it is acknowledged that the adoption of electric aircraft will not happen all of a sudden. In this respect, the development of a stochastic multi-stage approach that explicitly accounts for and supports the progressive roll-out of electric aircraft also makes a promising avenue for future research. Fourth, it might be interesting for future research to assess the integration and complementarity of regional electric aviation with the use of electric vertical take-off and landing (eVTOL) aircraft for last-mile/access-egress, or even for short routes between airports.

Appendix A. Proof of statements

A1. Proof of Proposition 1

Proof. Let us consider the three possible cases: (1) a charging base is located at i, i.e., $y_i = 1$; (2) no charging base is located at i and the closest charging base is located at a distance lower or equal than M^1, i.e., $y_i = 0$ and $\exists j \in \mathcal{N}_i : d_{ij} + \rho_j \leq M^1$; (3) no charging base is located at i and the closest charging base is farther than M^1, i.e., $y_i = 0$ and $\forall j \in \mathcal{N}_i : d_{ij} + \rho_j > M^1$.

Case 1. If $y_i = 1$, Constraint (11) would give $\rho_i = \min(0, \min_{j\in\mathcal{N}_i}(d_{ij} + \rho_j))$, which is zero because $(d_{ij} + \rho_j) > 0 \ \forall j \in \mathcal{N}_i$, by definition. On the other hand, the Constraints (12)–(16) would also give $\rho_i = 0$ because of the zero upper bound imposed by Constraints (12).

Case 2. If $y_i = 0$ and $\exists j \in \mathcal{N}_i : d_{ij} + \rho_j \leq M^1$, Constraint (11) gives $\rho_i = \min(M^1, \min_{j\in\mathcal{N}_i}(d_{ij} + \rho_j))$, which is $\min_{j\in\mathcal{N}_i}(d_{ij} + \rho_j)$. For the linear representation, Constraints (13) gives a tighter upper bound (i.e., $\rho_i \leq \min_{j\in\mathcal{N}_i}(d_{ij} + \rho_j)$) than M^1 that is given by Constraint (12). Hence, from Constraints (16), it has to be that the only w_{ij} set equal to 1 is for the $j = argmin_{j\in\mathcal{N}_i} d_{ij} + \rho_j$ which makes Constraints (14) enforce an equality $\rho_i = \min_{j\in\mathcal{N}_i}(d_{ij} + \rho_j)$—in combination with Constraints (13).

Case 3. If $y_i = 0$ and $\forall j \in \mathcal{N}_i : d_{ij} + \rho_j > M^1$, Constraint (11) gives $\rho_i = \min(M^1, \min_{j\in\mathcal{N}_i}(d_{ij} + \rho_j))$, which is M^1. The linear representation in Constraints (12)–(16) also give M^1: Constraint (12) gives a tighter upper bound (i.e., M^1) than $\min_{j\in\mathcal{N}_i}(d_{ij} + \rho_j)$ that is given by Constraints (13); in this case, Constraint (16) sets the auxiliary binary variables $w_{ij} = 0$ and $\chi_i = 1$ such that Constraint (15) is lifted to make $\rho_i = M^1$. Note that setting $w_{ij} = 1$ for $j \in \mathcal{N}_i$ would simply activate Constraints (14) (i.e., $\rho_i \geq d_{ij} + \rho_j$), which results into no feasible region between $\rho_i \leq M^1$ and $\rho_i \geq \min_{j\in\mathcal{N}_i}(d_{ij} + \rho_j)$. □

A2. Proof of Proposition 2

Proof. Let us note that $\tau \geq \min_{j'\in\mathcal{N}_i} d_{ij'}, \forall i \in \mathcal{N}$, as we filter out infeasible edges with a distance higher than the maximum range. Additionally, if no charging base is located at i, it follows that $\rho_i \geq \min_{j'\in\mathcal{N}_i} d_{ij'}$ from Constraints (12)–(16), resulting in two possible cases, based on the value of τ with respect to the minimum adjacent distance.

Case 1. If $\tau < 2\min_{j'\in\mathcal{N}_i} d_{ij'}$, then all adjacent edges to i are infeasible, since we cannot have a return trip from any adjacent node to i. Formally, this can be demonstrated from the edge feasibility constraint (4). First, note that $\tau < 2\min_{j'\in\mathcal{N}_i} d_{ij'}$ implies that $\rho_i > \tau - \min_{j'\in\mathcal{N}_i} d_{ij'}$. In fact, it can never be that $\rho_i \leq \tau - \min_{j'\in\mathcal{N}_i} d_{ij'}$ when $\tau < 2\min_{j'\in\mathcal{N}_i} d_{ij'}$ as this would be conflicting with $\rho_i \geq \min_{j'\in\mathcal{N}_i} d_{ij'}$. We now show that when $\rho_i > \tau - \min_{j'\in\mathcal{N}_i} d_{ij'}$, all edges adjacent to i are infeasible. Let us first assume that $\rho_i > \tau - \min_{j'\in\mathcal{N}_i} d_{ij'}$, which can be rewritten as $\rho_i = \tau - \min_{j'\in\mathcal{N}_i} d_{ij'} + \epsilon$ (where $\epsilon > 0$). Then, for any $j \in \mathcal{N}_i$ we have $d_{ij} + \tau - \min_{j'\in\mathcal{N}_i} d_{ij'} + \epsilon + \rho_j - M^3(1 - z_{ij}) \leq \tau$, which reduces to $d_{ij} - \min_{j'\in\mathcal{N}_i} d_{ij'} + \epsilon + \rho_j - M^3(1 - z_{ij}) \leq 0$. Then, since $d_{ij} - \min_{j'\in\mathcal{N}_i} d_{ij'} \geq 0$ for $j \in \mathcal{N}_i$, $\epsilon > 0$, and $\rho_j \geq 0$, it follows that $d_{ij} - \min_{j'\in\mathcal{N}_i} d_{ij'} + \epsilon > 0$ from which it must be that $z_{ij} = 0$.

Case 2. If $\tau \geq 2\min_{j'\in\mathcal{N}_i} d_{ij'}$, it can either be that $\rho_i > \tau - \min_{j'\in\mathcal{N}_i} d_{ij'}$ or $\rho_i \leq \tau - \min_{j'\in\mathcal{N}_i} d_{ij'}$. In the former subcase, we obtain that all adjacent edges are infeasible, following a similar reasoning as above in *Case* 1. By contrast, to complete the proof, we need to show that if $\rho_i \leq \tau - \min_{j'\in\mathcal{N}_i} d_{ij'}$, then there is at least an edge (i, j) that is not necessarily infeasible. Similar to above, we can rewrite $\rho_i = \tau - \min_{j'\in\mathcal{N}_i} d_{ij'} - \epsilon$ (where $\epsilon \geq 0$) and from Constraints (4) we obtain $d_{ij} - \min_{j'\in\mathcal{N}_i} d_{ij'} - \epsilon + \rho_j - M^3(1 - z_{ij}) \leq 0$ for any $j \in \mathcal{N}_j$. For the j such that $d_{ij} = \min_{j'\in\mathcal{N}_i} d_{ij'}$ it becomes $-\epsilon + \rho_j - M^3(1 - z_{ij}) \leq 0$. So, if a charger is located in j—which implies $\rho_j = 0$—then z_{ij} can be either 1 or 0.

□

Appendix B. Illustration of shortest path constraints and edge feasibility

Here, we illustrate the relationship between location of chargers and edge feasibility. Assume a simple network of 7 candidate airports (i.e., m, n, i, j, k, l, q) (represented in Fig. B.1, where three of them (m, i, and q) are selected as charging bases).

The constraints (12)–(16) set charging bases from candidate airports through binaries y_i, and compute the value of the shortest path ρ_i from each airport to an airport set as a charging base.

Table B.1
Illustration of the constraints for Fig. B.1. The lifted constraints are indicated with *.

Node	Constraints					Solution
	(12). $\rho_i \le M^1(1-y_i)$	(13). $\rho_i \le d_{ij}+\rho_j$	(14). $\rho_i \ge d_{ij}+\rho_j - M^2(1-w_{ij})$	(15). $\rho_i \ge M^1\chi_i$	(16). $\sum_{j\in\mathcal{N}_j} w_{ij}+y_i+\chi_i=1$	
m	$\rho_m \le M^1(1-y_m)[=0]$	$\rho_m \le 4+\rho_n[=6]$ $\rho_m \le 5+\rho_i[=5]$	$\rho_m \ge 4+\rho_n - M^2(1-w_{mn})*$ $\rho_m \ge 5+\rho_i - M^2(1-w_{mi})*$	$\rho_m \ge M^1\chi_m[=0]$	$w_{mn}+w_{mi}+y_m+\chi_m=1$	$y_m=1$ $\rho_m=0$
i	$\rho_i \le M^1(1-y_i)[=0]$	$\rho_i \le 2+\rho_n[=4]$ $\rho_i \le 2+\rho_j[=4]$ $\rho_i \le 5+\rho_m[=5]$	$\rho_i \ge 2+\rho_n - M^2(1-w_{in})*$ $\rho_i \ge 2+\rho_j - M^2(1-w_{ij})*$ $\rho_i \ge 5+\rho_m - M^2(1-w_{im})*$	$\rho_i \ge M^1\chi_i[=0]$	$w_{in}+w_{ij}+w_{im}+y_i+\chi_i=1$	$y_i=1$ $\rho_i=0$
q	$\rho_q \le M^1(1-y_q)[=0]$	$\rho_q \le 1+\rho_l[=2]$	$\rho_q \ge 1+\rho_l - M^2(1-w_{ql})*$	$\rho_q \ge M^1\chi_q[=0]$	$w_{ql}+y_q+\chi_q=1$	$y_q=1$ $\rho_q=0$
n	$\rho_n \le M^1(1-y_n)[=M^1]$	$\rho_n \le 4+\rho_m[=4]$ $\rho_n \le 2+\rho_i[=2]$	$\rho_n \ge 4+\rho_m - M^2(1-w_{nm})*$ $\rho_n \ge 2+\rho_i - M^2(1-w_{ni})[=2]$	$\rho_n \ge M^1\chi_n[=0]$	$w_{nm}+w_{ni}+y_n+\chi_n=1$	$w_{ni}=1$ $\rho_n=2$
l	$\rho_l \le M^1(1-y_l)[=M^1]$	$\rho_l \le 2+\rho_j[=4]$ $\rho_l \le 1+\rho_q[=1]$	$\rho_l \ge 2+\rho_j - M^2(1-w_{lj})*$ $\rho_l \ge 1+\rho_q - M^2(1-w_{lq})[=1]$	$\rho_l \ge M^1\chi_l[=0]$	$w_{lj}+w_{lq}+y_l+\chi_l=1$	$w_{lq}=1$ $\rho_l=1$
j	$\rho_j \le M^1(1-y_j)[=M^1]$	$\rho_j \le 2+\rho_i[=2]$ $\rho_j \le 2+\rho_k[=6]$ $\rho_j \le 2+\rho_l[=3]$	$\rho_j \ge 2+\rho_i - M^2(1-w_{ji})[=2]$ $\rho_j \ge 7+\rho_k - M^2(1-w_{jk})*$ $\rho_j \ge 2+\rho_l - M^2(1-w_{jl})*$	$\rho_j \ge M^1\chi_j[=0]$	$w_{ji}+w_{jk}+w_{jl}+y_j+\chi_j=1$	$w_{ji}=1$ $\rho_j=2$
k	$\rho_k \le M^1(1-y_k)[=M^1]$	$\rho_k \le 2+\rho_j[=4]$	$\rho_k \ge 2+\rho_j - M^2(1-w_{kj})[=4]$	$\rho_k \ge M^2\chi_k[=0]$	$w_{kj}+y_k+\chi_k=1$	$w_{kj}=1$ $\rho_k=4$

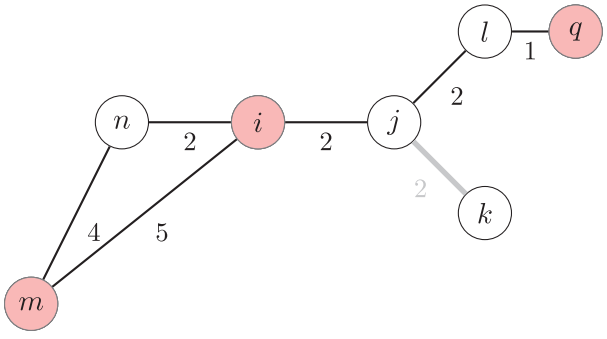

Fig. B.1. Illustration of the relationship between location of chargers and edge feasibility. Assume a maximum range on a single charge $\tau = 6$. The activated airport is colored light-red. Edge (j,k) is infeasible. (For interpretation of the references to color in this figure legend, the reader is referred to the web version of this article.)

First, we illustrate the calculation of the value of shortest path for any node i (i.e., ρ_i), given the values of y_i. For any airport selected as a charging base, the value of shortest path is zero. Take airport m as an example. The fact that $y_m = 1$ directly implies $w_{mn}, w_{mi}, \chi_i = 0$ from Constraint (16). Constraints (12) and (15) thus become $\rho_m \le 0$ and $\rho_m \ge 0$, respectively, hence setting $\rho_m = 0$. The calculation of the value of shortest path for airports i and q follows a similar manner. On the other hand, the calculation of the value of shortest path for any airport not selected as a charging base proceeds as follows. Take airport n as an example, i.e., $y_n = 0$. First, note that Constraint (12) is lifted, i.e., $\rho_n \le M^1$. Then, given that the two adjacent airports of n (i.e., m and i) are selected as charging bases, we obtain that $y_m, y_i = 1$, and $\rho_m, \rho_i = 0$. In turn, Constraints (13) become $\rho_n \le 2$ (in relation to i) and $\rho_n \le 4$ (in relation to m), which means that $\rho_n \le 2$ because $2 < 4 < M^1$. Constraint (15) is deactivated by $\chi_n = 0$ since setting it to one would create an infeasible system of inequalities (i.e., $\rho_n \ge M^1$ from Constraint (15) and $\rho_n \le 2$ from Constraints (13)). By Constraint (16), $y_n, \chi_n = 0$ then yields $w_{nm} + w_{ni} = 1$. Finally, from Constraints (14), it has to be that $w_{nm} = 0$ and $w_{ni} = 1$, enforcing $\rho_n \ge 2$ and ultimately yielding $\rho_n = 2$. The calculation of the value of shortest path for airports j, l and k follows a similar manner, as illustrated in Table B.1.

Second, we illustrate the computation of the feasibility of an edge using Constraint (4) that takes into account the maximum range on a single charge τ. In Fig. B.1, edge (j,l) is feasible; we have that $\rho_j + d_{jl} + \rho_l = 2 + 2 + 1$, which is < 6, hence there is not need to activate big-M parameters and z_{ij} can be either 0 or 1. It is easy to see that the same holds for all the other edges except (j,k). Given the charger setting, there is no aircraft routing (i.e., a sequence of arcs linking two charging bases) through arc (j,k) with an overall length lower than the maximum range, such that it is impossible to operate arc z_{ij}. Mathematically, for (j,k) we obtain that $\rho_j + d_{jk} + \rho_k = 2 + 2 + 4$ is > 6. Hence z_{jk} needs to be 1 to satisfy Constraint (4).

Appendix C. Illustration of need for χ_i variables

Here, we illustrate the importance of auxiliary variable χ_i. Consider a simple network as in Fig. C.2, with airport d in the major destination to be reached. Assume candidate airports n and m form a sub-network, which cannot be linked to the destination due to range limitations.

In this case, the practical solution is to neither locate chargers at n nor m. However, without auxiliary variables χ_i, this is not possible and the model would be forced to locate a charger at n and/or m. To clarify, let us assume no use of χ_i and that no charger is located in the $m-n$ sub-network (i.e., $y_n = y_m = 0$). In turn, this implies that $w_{nm} = w_{mn} = 1$ by Constraints (16), ultimately yielding the following system of equations (Constraints (13) and (14)):

$$\begin{cases} \rho_n \le 4 + \rho_m \\ \rho_m \le 4 + \rho_n \\ \rho_n \ge 4 + \rho_m \\ \rho_m \ge 4 + \rho_n \end{cases} \tag{C.1}$$

which is impossible to solve. Hence, the model would either locate a charger in n or m to verify all the constraints. The use of variables χ_n and χ_m avoids such unpractical solutions. Indeed, in case the shortest path is larger than M^1, it allows to set $\chi_n = \chi_m = 1$ such that $y_n = y_m = w_{nm} = w_{mn} = 0$.

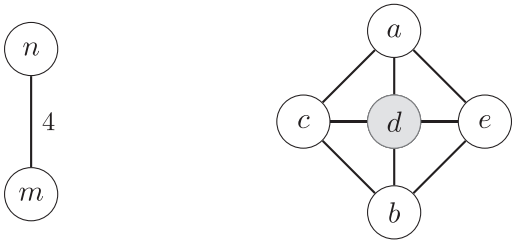

Fig. C.2. Simple network with a disjoint sub-network. The destination airport is colored gray.

References

Åkerman, J., Kamb, A., Larsson, J., & Nässén, J. (2021). Low-carbon scenarios for long-distance travel 2060. *Transportation Research Part D: Transport and Environment, 99*, 103010.

Andersson, B. (2019). Flygutredning 2019–2023. Utredning inför beslut om allmän trafikplikt. In *Trafikverket publications: vol. 117*. Trafikverket, Sweden.

Angelelli, E., Mansini, R., & Speranza, M. (2007). Kernel search: A heuristic framework for MILPproblems with binary variables. *Technical report 2007-04-56*. Department of Electronics for Automation, University of Brescia.

Angelelli, E., Mansini, R., & Speranza, M. G. (2010). Kernel search: A general heuristic for the multi-dimensional knapsack problem. *Computers and Operations Research, 37*(11), 2017–2026.

Barnhart, C., Boland, N. L., Clarke, L. W., Johnson, E. L., Nemhauser, G. L., & Shenoi, R. G. (1998a). Flight string models for aircraft fleeting and routing. *Transportation Science, 32*(3), 208–220.

Barnhart, C., Johnson, E. L., Nemhauser, G. L., Savelsbergh, M. W., & Vance, P. H. (1998b). Branch-and-price: Column generation for solving huge integer programs. *Operations Research, 46*(3), 316–329.

Barzkar, A., & Ghassemi, M. (2020). Electric power systems in more and all electric aircraft: a review. *IEEE Access, 8*, 169314–169332 IEEE.

Baumeister, S., Leung, A., & Ryley, T. (2020). The emission reduction potentials of first generation electric aircraft (FGEA) in Finland. *Journal of Transport Geography, 85*, 102730.

Birolini, S., Malighetti, P., Redondi, R., & Deforza, P. (2019). Access mode choice to low-cost airports: Evaluation of new direct rail services at Milan-Bergamo airport. *Transport Policy, 73*, 113–124. https://doi.org/10.1016/j.tranpol.2018.10.008.

Bråthen, S., & Eriksen, K. S. (2018). Regional aviation and the PSO system–level of service and social efficiency. *Journal of Air Transport Management, 69*, 248–256.

Church, R., & ReVelle, C. (1974). The maximal covering location problem. In *Papers of the regional science association: vol. 32* (pp. 101–118). Springer-Verlag.

Cornuéjols, G., Sridharan, R., & Thizy, J.-M. (1991). A comparison of heuristics and relaxations for the capacitated plant location problem. *European Journal of Operational Research, 50*(3), 280–297.

Daskin, M. S. (2011). *Network and discrete location: Models, algorithms, and applications*. John Wiley & Sons.

D'Alfonso, T., Jiang, C., & Bracaglia, V. (2016). Air transport and high-speed rail competition: Environmental implications and mitigation strategies. *Transportation Research Part A: Policy and Practice, 92*, 261–276.

EASA (2019). European aviation environmental report 2019.

Eviation (2021). Eviation alice(available at: eviation.co/aircraft).

Fageda, X., Suárez-Alemán, A., Serebrisky, T., & Fioravanti, R. (2018). Air connectivity in remote regions: A comprehensive review of existing transport policies worldwide. *Journal of Air Transport Management, 66*, 65–75.

Filippi, C., Guastaroba, G., Huerta-Muñoz, D., & Speranza, M. (2021). A kernel search heuristic for a fair facility location problem. *Computers and Operations Research, 132*, 105292.

Filippi, C., Guastaroba, G., & Speranza, M. (2016). A heuristic framework for the bi-objective enhanced index tracking problem. *Omega, 65*, 122–137.

Graham, B. (1997). Regional airline services in the liberalized European Union single aviation market. *Journal of Air Transport Management, 3*(4), 227–238.

Grewe, V., Rao, A. G., Grönstedt, T., Xisto, C., Linke, F., Melkert, J., … Christie, S., et al., (2021). Evaluating the climate impact of aviation emission scenarios towards the paris agreement including COVID-19 effects. *Nature Communications, 12*(1), 1–10.

Guastaroba, G., Savelsbergh, M., & Speranza, M. G. (2017). Adaptive kernel search: A heuristic for solving mixed integer linear programs. *European Journal of Operational Research, 263*(3), 789–804.

Guastaroba, G., & Speranza, M. G. (2012). Kernel search: An application to the index tracking problem. *European Journal of Operational Research, 217*(1), 54–68.

Guastaroba, G., & Speranza, M. G. (2014). A heuristic for BILP problems: The single source capacitated facility location problem. *European Journal of Operational Research, 238*(2), 438–450.

Gudmundsson, S. V., Cattaneo, M., & Redondi, R. (2021). Forecasting temporal world recovery in air transport markets in the presence of large economic shocks: The case of COVID-19. *Journal of Air Transport Management, 91*, 102007.

Hagberg, A., Swart, P., & S Chult, D. (2008). Exploring network structure, dynamics, and function using NetworkX. *Technical report*. Los Alamos National Lab.(LANL), Los Alamos, NM (United States).

Heart Aerospace (2021). Heart Aerospace(available at: https://heartaerospace.com/faq).

Hiermann, G., Puchinger, J., Ropke, S., & Hartl, R. F. (2016). The electric fleet size and mix vehicle routing problem with time windows and recharging stations. *European Journal of Operational Research, 252*(3), 995–1018.

Hosseini, M., & MirHassani, S. (2015). Refueling-station location problem under uncertainty. *Transportation Research Part E: Logistics and Transportation Review, 84*, 101–116.

Hung, Y.-C., Lok, H. P., & Michailidis, G. (2022). Optimal routing for electric vehicle charging systems with stochastic demand: A heavy traffic approximation approach. *European Journal of Operational Research, 299*(2), 526–541.

IATA (2021). Aircraft technology roadmap to 2050. *Technical Report*. OECD. https://www.iata.org/contentassets/8d19e716636a47c184e7221c77563c93/Technology-roadmap-2050.pdf.

ICAO (2021). International Standards and Recommended Practices: Operation of Aircraft: Annex 6 to the Convention on International Civil Aviation. Accessed 2022-09-19, https://standart.aero/en/icao/book/annex-6-p-1-operation-of-aircraft-part-i-international-commercial-air-transport-aeroplanes-ed-11-en-12219-2021-02-15.

Justin, C. Y., Payan, A. P., Briceno, S. I., German, B. J., & Mavris, D. N. (2020). Power optimized battery swap and recharge strategies for electric aircraft operations. *Transportation Research Part C: Emerging Technologies, 115*, 102605.

Justin, C. Y., Payan, A. P., & Mavris, D. N. (2022). Integrated fleet assignment and scheduling for environmentally friendly electrified regional air mobility. *Transportation Research Part C: Emerging Technologies, 138*, 103567.

Kınay, Ö. B., Gzara, F., & Alumur, S. A. (2021). Full cover charging station location problem with routing. *Transportation Research Part B: Methodological, 144*, 1–22.

Kinene, A., Granberg, T. A., Birolini, S., Adler, N., Polishchuk, V., & Skoglund, J.-M. (2022). An auction framework for assessing the tendering of subsidised routes in air transportation. *Transportation Research Part A: Policy and Practice, 159*, 320–337.

Lamanna, L., Mansini, R., & Zanotti, R. (2022). A two-phase kernel search variant for the multidimensional multiple-choice knapsack problem. *European Journal of Operational Research, 297*(1), 53–65.

Mak, H.-Y., Rong, Y., & Shen, Z.-J. M. (2013). Infrastructure planning for electric vehicles with battery swapping. *Management Science, 59*(7), 1557–1575.

Maniezzo, V., Boschetti, M. A., & Stützle, T. (2021). Kernel search. In *Matheuristics* (pp. 189–197). Springer.

Nava, C. R., Meleo, L., Cassetta, E., & Morelli, G. (2018). The impact of the EU-ETS on the aviation sector: Competitive effects of abatement efforts by airlines. *Transportation Research Part A: Policy and Practice, 113*, 20–34.

OECD (2021). Aligning short-term recovery measures with longer-term climate and environmental objectives in Eastern Europe, Caucasus and Central Asia. *Technical report*. OECD. https://www.oecd.org/environment/outreach/ENVEPOCEAP(2021)4-GreenRecoveryEECCA.pdf.

Our Airports (2021). Open data@OurAirports. Accessed 2021-11-02, https://ourairports.com/data/.

Paleari, S., Redondi, R., & Malighetti, P. (2010). A comparative study of airport connectivity in China, Europe and US: Which network provides the best service to passengers? *Transportation Research Part E: Logistics and Transportation Review, 46*(2), 198–210.

Patterson, M. D., Derlaga, J. M., & Borer, N. K. (2016). High-lift propeller system configuration selection for NASA's SCEPTOR distributed electric propulsion flight demonstrator. In *16th AIAA aviation technology, integration, and operations conference* (p. 3922).

Rajendran, S., & Srinivas, S. (2020). Air taxi service for urban mobility: A critical review of recent developments, future challenges, and opportunities. *Transportation Research Part E: Logistics and Transportation Review, 143*, 102090.

Reimers, J. O. (2018). Introduction of electric aviation in Norway. *Technical report*. https://avinor.no/contentassets/c29b7a7ec1164e5d8f7500f8fef810cc/introduction-of-electric-aircraft-in-norway.pdf.

Rohacs, J., & Rohacs, D. (2020). Energy coefficients for comparison of aircraft supported by different propulsion systems. *Energy, 191*, 116391.

Salucci, F., Riboldi, C. E., Trainelli, L., & Rolando, A. (2020). Optimal recharging infrastructure sizing and operations for a regional airport. In *1st aerospace Europe conference (AEC 2020)* (pp. 1–8).

Sayed, E., Abdalmagid, M., Pietrini, G., Sa'adeh, N.-M., Callegaro, A. D., Goldstein, C., & Emadi, A. (2021). Review of electric machines in more/hybrid/turbo electric aircraft. *IEEE Transactions on Transportation Electrification, 7*(4), 2976–3005.

Schäfer, A. W., Barrett, S. R., Doyme, K., Dray, L. M., Gnadt, A. R., Self, R., … Torija, A. J. (2019). Technological, economic and environmental prospects of all-electric aircraft. *Nature Energy, 4*(2), 160–166.

Schwab, A., Thomas, A., Bennett, J., Robertson, E., & Cary, S. (2021). Electrification of aircraft: Challenges, barriers, and potential impacts. *Technical report*. National Renewable Energy Lab. (NREL), Golden, CO (United States).

Sedgewick, R. (2001). *Algorithms in C, part 5: Graph algorithms*. Pearson Education.

Sharma, A., Jakhar, S. K., & Choi, T.-M. (2021). Would CORSIA implementation bring carbon neutral growth in aviation? A case of US full service carriers. *Transportation Research Part D: Transport and Environment, 97*, 102839.

Tatem, A. J. (2017). Worldpop, open data for spatial demography. *Scientific Data, 4*(1), 1–4.

TrafikAnalys (2020). Elflyg—början på en spännande resa. *Technical report*. TrafikAnalys, Sweden. https://www.trafa.se/globalassets/rapporter/2020/rapport-2020_12-elflyg_borjan-pa-en-spannande-resa.pdf.

Trainelli, L., Salucci, F., Riboldi, C. E., Ronaldo, A., & Bigoni, F. (2021). Optimal sizing and operation of airport infrastructures in support of electric-powered aviation. *Aerospace, 8*(2), 40.

Vespermann, J., & Wald, A. (2011). Much ado about nothing?—An analysis of economic impacts and ecologic effects of the EU-emission trading scheme in the aviation industry. *Transportation Research Part A: Policy and Practice, 45*(10), 1066–1076.

Willey, L. C., & Salmon, J. L. (2021). A method for urban air mobility network design using hub location and subgraph isomorphism. *Transportation Research Part C: Emerging Technologies, 125*, 102997.

Williams, G., & Pagliari, R. (2004). A comparative analysis of the application and use of public service obligations in air transport within the EU. *Transport Policy, 11*(1), 55–66.

Yang, Z., Chen, H., Chu, F., & Wang, N. (2019). An effective hybrid approach to the two-stage capacitated facility location problem. *European Journal of Operational Research, 275*(2), 467–480.